Pseudo-Marginal Hamiltonian Monte Carlo with Efficient Importance Sampling

Kjartan Kloster Osmundsen [a,*]
Tore Selland Kleppe [a]
Roman Liesenfeld [b]

December 20, 2018

[a] Department of Mathematics and Physics, University of Stavanger, Norway

[b] Institute of Econometrics and Statistics, University of Cologne, Germany

Abstract

The joint posterior of latent variables and parameters in Bayesian hierarchical models often has a strong nonlinear dependence structure, thus making it a challenging target for standard Markov-chain Monte-Carlo methods. Pseudo-marginal methods aim at effectively exploring such target distributions, by marginalizing the latent variables using Monte-Carlo integration and directly targeting the marginal posterior of the parameters. We follow this approach and propose a generic pseudo-marginal algorithm for efficiently simulating from the posterior of the parameters. It combines efficient importance sampling, for accurately marginalizing the latent variables, with the recently developed pseudo-marginal Hamiltonian Monte Carlo approach. We illustrate our algorithm in applications to dynamic state space models, where it shows a very high simulation efficiency even in challenging scenarios with complex dependence structures.

Keywords: Hamiltonian Monte Carlo, Efficient importance sampling, Bayesian hierarchical models, State space models

1 Introduction

Standard Markov-Chain Monte-Carlo (MCMC) methods are often ineffective in exploring target distributions with complex dependence structures. Such distributions can arise, for instance, as the joint posterior of latent variables and parameters in the class of Bayesian hierarchical models. This class includes, amongst others, dynamic non-Gaussian and/or nonlinear state-space models (SSMs). According to Betancourt and Girolami

---

*Corresponding author. E-mail address: kjartan.k.osmundsen@uis.no

(2015), existing MCMC methods for Bayesian inference in such hierarchical models can be classified into Gibbs sampling algorithms alternately updating the latent variables and parameters, methods that update latent variables and parameters jointly, and pseudo-marginal methods. Gibbs sampling is widely used, in part due to its simple implementation (Liu, 2001; Robert and Casella, 2004). However, a naive implementation updating latent variables in one block and model parameters in another block can suffer from a very slow exploration of the target distribution if this distribution implies a strong correlation of the variables in the two blocks. Methods that update latent variables and parameters jointly avoid this correlation problem of Gibbs sampling. One such approach for joint updates is to use Hamiltonian Monte Carlo (HMC) methods (see, Kleppe, 2018b, and references therein). However, they critically require update proposals which are properly aligned with the local geometry of the target, the generation of which can be computationally demanding for complex high-dimensional joint posteriors of the parameters and latent variables and needs a high degree of expertise to adapt it to the specific application.

Pseudo-marginal methods directly target the marginal posterior of the parameters. They do so by marginalizing the latent variables using Monte Carlo (MC) integration and typically utilizing Metropolis Hastings (MH) schemes for updating the parameters (Fernandez-Villaverde and Rubio-Ramirez, 2007; Andrieu et al., 2010; Flury and Shephard, 2011; Pitt et al., 2012). This approach also bypasses the correlation problem of Gibbs sampling, but relies on the ability to produce an unbiased and accurate low-variance MC estimate for the analytically intractable marginal posterior of the parameters. For SSMs and related latent variable models, sequential Monte Carlo (SMC) methods, also known as particle filters, can be used to produce such unbiased estimates while being relatively straightforward to implement (see e.g. Doucet et al., 2001). However, for high-dimensional models with a large number of latent variables, producing accurate estimates via particle filters can often be extremely computationally demanding (Flury and Shephard, 2011). Moreover, as for any MH scheme, it can be difficult to select an efficient proposal distribution for updating the parameters and its tuning may be difficult if the MC estimates for the marginal posterior are noisy and/or contain many discontinuities.

In this paper, we propose a new pseudo-marginal algorithm for Bayesian hierarchical models. It consists of a combination of the pseudo-marginal HMC (PM-HMC) approach of Lindsten and Doucet (2016) and the efficient importance sampling (EIS) algorithm (Liesenfeld and Richard, 2003; Richard and Zhang, 2007). The PM-HMC approximates the ideal HMC targeting the marginal posterior of the parameters. This is done by replacing in the (exact) HMC target the marginal posterior by an unbiased MC importance sampling (IS) estimate. This approach aims at taking advantage of the respective strength of pseudo-marginal schemes and HMCs: Being a pseudo-marginal algorithm it avoids operating on the joint posterior distribution of the parameters and latent variables; and as an HMC it utilizes the local curvature of the target for producing

MCMC updates, thereby avoiding the slow exploration of the target that often results from standard MH updating schemes. To preserve the invariant distribution of interest, the HMC target distribution is augmented to include all the auxiliary random variables that need to be generated to obtain an MC IS estimate of the marginal posterior. For implementation, this estimate must be a smooth function of both the auxiliary variables and the parameters, and for good performance, its variance should not exceed some critical value. These requirements appear to substantially reduce the range of potential applications of the PM-HMC approach. For instance, particle filters used in other pseudo-marginal methods define MC estimators for the marginal posterior which are typically discontinuous functions of their auxiliary variables and the parameters (see, e.g., Malik and Pitt, 2011), while 'brute force' IS estimators as used by Lindsten and Doucet (2016) can suffer from a prohibitively large variance when applied to high-dimensional dynamic latent variable models (see, e.g., Danielsson, 1994).

In order to extend the range of its potential applications, we propose to combine the PM-HMC approach with the EIS algorithm. EIS provides a generic approach for constructing IS densities aiming at minimizing the variance of MC estimates for target integrals like marginal likelihood functions (and resulting marginal posteriors) in the presence of latent variables. As such, it has been successfully applied to the analysis for a wide range of non-Gaussian and/or non-linear latent variable models, including high-dimensional dynamic ones (see e.g. Liesenfeld and Richard, 2003, 2006, 2008; Bauwens and Galli, 2009; DeJong et al., 2012; Kleppe and Liesenfeld, 2014; Kleppe et al., 2014; Moura and Turatti, 2014; Scharth and Kohn, 2016; Grothe et al., 2018; Liesenfeld et al., 2016, 2017). Since EIS not only produces highly accurate MC likelihood estimates for a large class of latent variable models, but also allows to construct those estimates as smooth functions of the parameters and auxiliary variables, it can be expected to be well-suited for generating PM-HMC targets that allow for an efficient exploration of marginal posteriors for a broad range of applications. A further attractive feature of EIS is that it also provides MC approximations of the maximum posteriori probability (MAP) values of the parameters and negative Hessians, which can be usefully applied for tuning the PM-HMC (see Gelman et al., 2014, chapter 13.3).

The rest of the paper is organized as follows. In Section 2 we briefly outline the HMC and PM-HMC approach. Section 3 details how EIS can be incorporated into PM-HMC. A simulation study using the proposed methodology is presented in Section 4. A more detailed analysis of PM-HMC when only a single draw is used in the EIS sampler is provided in Section 5, before final discussion is given in Section 6.

2 HMC and the PM-HMC Approach

This section briefly outlines the HMC principle (Section 2.1) and the PM-HMC method of Lindsten and Doucet (2016) (Section 2.2). In what follows, we use $\mathcal{N}(\mathbf{x}|\boldsymbol{\mu}, \boldsymbol{\Sigma})$ to denote the probability density function of a $N(\boldsymbol{\mu}, \boldsymbol{\Sigma})$ random vector evaluated at $\mathbf{x}$, while $\nabla_{\mathbf{z}}$ and $\nabla_{\mathbf{z}}^2$ are used, respectively, for the gradient and Hessian operator with respect to the vector $\mathbf{z}$.

2.1 HMC Principle

During the last decade, HMC introduced by Duane et al. (1987) has been extensively used as a general purpose MCMC method, often applied for simulating from posterior distributions arising in Bayesian models (Neal, 2011). HMC offers the advantage of producing close to perfectly mixing MCMC chains by using the dynamics of a synthetic Hamiltonian system as proposal mechanism. An HMC implementation which is used in many practical applications is that based on the no-U-turn sampler of Hoffman and Gelman (2014) which is available in the popular Bayesian modeling software Stan (Stan Development Team, 2017).

Suppose one seeks to sample from an analytically intractable target distribution with density kernel $\tilde{\pi}(\mathbf{q})$, $\mathbf{q} \in \Omega \subseteq \mathbb{R}^s$. To this end, HMC takes the variable of interest $\mathbf{q}$ as the 'position coordinate' of a Hamiltonian system, which is complemented by an (artificial) 'momentum variable' $\mathbf{p} \in \mathbb{R}^s$. The corresponding Hamiltonian function specifying the total energy of the dynamical system is given by

$$H(\mathbf{q}, \mathbf{p}) = -\log \tilde{\pi}(\mathbf{q}) + \frac{1}{2}\mathbf{p}'\mathbf{M}^{-1}\mathbf{p},$$

where $\mathbf{M} \in \mathbb{R}^{s \times s}$ is a symmetric, positive definite 'mass matrix' representing an HMC tuning parameter. For near-Gaussian target distributions, for instance, setting $\mathbf{M}$ close to the precision matrix of the target ensures the best performance. The law of motions under the dynamic system specified by the Hamiltonian H is determined by Hamilton's equations given by

$$\frac{d}{dt}\mathbf{p}(t) = -\nabla_{\mathbf{q}}H\left(\mathbf{q}(t), \mathbf{p}(t)\right), \qquad \frac{d}{dt}\mathbf{q}(t) = \nabla_{\mathbf{p}}H\left(\mathbf{q}(t), \mathbf{p}(t)\right). \tag{1}$$

It can be shown that the dynamics associated with the Hamilton's equations preserves both the Hamiltonian (i.e. $dH\left(\mathbf{q}(t), \mathbf{p}(t)\right)/dt = 0$) and the Boltzmann distribution

$$\pi(\mathbf{q}, \mathbf{p}) \propto \exp\{-H(\mathbf{q}, \mathbf{p})\} \propto \tilde{\pi}(\mathbf{q})\,\mathcal{N}(\mathbf{p}|\mathbf{0}_s, \mathbf{M}).$$

This implies that if $[\mathbf{q}(t), \mathbf{p}(t)] \sim \pi(\mathbf{q}, \mathbf{p})$, then $[\mathbf{q}(t+\tau), \mathbf{p}(t+\tau)] \sim \pi(\mathbf{q}, \mathbf{p})$ for any (scalar) time increment τ.

Based on this property, a valid MCMC scheme for generating $\{\mathbf{q}^{(k)}\}_k \sim \tilde{\pi}(\mathbf{q})$ would be to alternate between the following two steps: (i) Sample a new momentum $\mathbf{p}^{(k)} \sim N(\mathbf{0}_s, \mathbf{M})$; and (ii) use the Hamiltonian's equations (1) to propagate $[\mathbf{q}(0), \mathbf{p}(0)] = [\mathbf{q}^{(k)}, \mathbf{p}^{(k)}]$ for some increment τ to obtain $[\mathbf{q}(\tau), \mathbf{p}(\tau)] = [\mathbf{q}^{(k+1)}, \mathbf{p}^*]$ and discard $\mathbf{p}^*$. However, for all but very simple scenarios (like those with a Gaussian target $\tilde{\pi}(\mathbf{q})$) the transition dynamics according to (1) does not admit closed-form solution, in which case it is necessary to rely on numerical integrators for an approximative solution. Provided that the numerical integrator used for that purpose is symplectic, the numerical approximation error can be exactly corrected by introducing an accept-reject (AR) step, which uses the Hamiltonian to compare the total energy of the new proposal for the pair $(\mathbf{q}, \mathbf{p})$ with that of the old pair inherited from the previous MCMC step (see, e.g., Neal, 2011). The most commonly used symplectic integrator is the Störmer-Verlet or leap-frog integrator (see, e.g., Leimkuhler and Reich, 2004; Neal, 2011), but also more elaborate symplectic integrators have been developed with the aim of further improving efficiency of HMC (Blanes et al., 2014; Mannseth et al., 2018). When implementing numerical integrators with AR-corrections it is critical that the selection of the step size accounts for the inherent trade-off between the computing time required for generating AR proposals and their quality reflected by their corresponding acceptance rates. $(\mathbf{q}, \mathbf{p})$-proposals generated by using small (big) step sizes tend to be computationally expensive (cheap) but imply a high (low) level of energy preservation and thus high (low) acceptance rates.

2.2 PM-HMC

Consider a stochastic model for a collection of observed data $\mathbf{y}$ involving a collection of latent variables $\mathbf{x}$ and a vector of parameters $\boldsymbol{\theta} \in \mathbb{R}^d$ with prior density $p(\boldsymbol{\theta})$. The conditional likelihood for $\mathbf{y}$ given a value for $\mathbf{x}$ is denoted by $p(\mathbf{y}|\mathbf{x}, \boldsymbol{\theta})$ and the prior for $\mathbf{x}$ by $p(\mathbf{x}|\boldsymbol{\theta})$. This latent variable model is assumed to be nonlinear and/or non-Gaussian so that both the joint posterior for $(\mathbf{x}, \boldsymbol{\theta})$ as well as the marginal posterior for $\boldsymbol{\theta}$ are analytically intractable.

As mentioned above, the joint posterior for $(\mathbf{x}, \boldsymbol{\theta})$ under such a latent variable model, given by $p(\mathbf{x}, \boldsymbol{\theta}|\mathbf{y}) \propto p(\mathbf{y}|\mathbf{x}, \boldsymbol{\theta})p(\mathbf{x}|\boldsymbol{\theta})p(\boldsymbol{\theta})$, can have a complex dependence structure. This prevents that it can be efficiently explored by using a standard HMC for $\mathbf{q} = (\mathbf{x}', \boldsymbol{\theta}')'$ as described in Section 2.1, or any other conventional MCMC scheme. The pseudo-marginal approach bypasses this problem by directly targeting the marginal posterior of the parameters

$$p(\boldsymbol{\theta}|\mathbf{y}) \propto p(\mathbf{y}|\boldsymbol{\theta})p(\boldsymbol{\theta}), \tag{2}$$

where

$$p(\mathbf{y}|\boldsymbol{\theta}) = \int p(\mathbf{y}|\mathbf{x}, \boldsymbol{\theta})p(\mathbf{x}|\boldsymbol{\theta})d\mathbf{x}. \tag{3}$$

Without having a closed-form solution, the likelihood integral (3) needs to be approximated by numerical methods such as MC integration procedures like IS or particle filters. An IS approach approximating such likelihood functions for maximum-likelihood analyses is found, e.g., in Durbin and Koopman (2012, part II), and particle filter likelihood estimation in Bayesian MCMC analyses, e.g., in Andrieu et al. (2010).

The PM-HMC of Lindsten and Doucet (2016) relies on such MC estimation of the likelihood in (3) in order to exactly approximate the ideal HMC targeting the marginal posterior defined in (2). For this, the MC estimator for the likelihood function, denoted by $\hat{p}(\mathbf{y}|\boldsymbol{\theta}, \mathbf{u})$, is required to be a smooth function in the parameters $\boldsymbol{\theta}$ and the auxiliary random variables $\mathbf{u} \in \mathbb{R}^D$ which are used to produce the estimate. This estimate is supposed to be unbiased, i.e., $E_{\mathbf{u}}[\hat{p}(\mathbf{y}|\boldsymbol{\theta}, \mathbf{u})] = p(\mathbf{y}|\boldsymbol{\theta}) \, \forall \, \boldsymbol{\theta}$, and without loss of generality it is also assumed that $\mathbf{u} \sim N(\mathbf{0}_D, \mathbf{I}_D)$. The smoothness is required as the Hamiltonian transition dynamics of the PM-HMC (as provided in (6) below) relies on gradients of $\log[\hat{p}(\mathbf{y}|\boldsymbol{\theta}, \mathbf{u})]$.

The exact approximation of the ideal HMC is achieved by replacing in the targeted posterior (2) the likelihood $p(\mathbf{y}|\boldsymbol{\theta})$ by its unbiased MC estimate $\hat{p}(\mathbf{y}|\boldsymbol{\theta}, \mathbf{u})$, and then to correct the estimation error in the resulting estimated target by augmenting it to include the auxiliary variables $\mathbf{u}$. The resulting joint density for $\boldsymbol{\theta}$ and $\mathbf{u}$ is given by

$$\bar{\pi}(\boldsymbol{\theta}, \mathbf{u}) \propto \hat{p}(\mathbf{y}|\boldsymbol{\theta}, \mathbf{u})p(\boldsymbol{\theta})\mathcal{N}(\mathbf{u}|\mathbf{0}_D, \mathbf{I}_D), \tag{4}$$

and admits under the unbiasedness assumption for $\hat{p}(\mathbf{y}|\boldsymbol{\theta}, \mathbf{u})$ the exact target $p(\boldsymbol{\theta}|\mathbf{y})$ as the marginal. The PM-HMC then obtains as a standard HMC for simulating the random vector $\mathbf{q} = (\boldsymbol{\theta}', \mathbf{u}')'$ from the augmented target density (4). The corresponding extended Hamiltonian is

$$H(\boldsymbol{\theta}, \mathbf{u}, \mathbf{p}_{\boldsymbol{\theta}}, \mathbf{p}_{\mathbf{u}}) = -\log \hat{p}(\mathbf{y}|\boldsymbol{\theta}, \mathbf{u}) - \log p(\boldsymbol{\theta}) + \frac{1}{2}\mathbf{u}'\mathbf{u} + \frac{1}{2}\mathbf{p}_{\boldsymbol{\theta}}'\mathbf{M}_{\boldsymbol{\theta}}^{-1}\mathbf{p}_{\boldsymbol{\theta}} + \frac{1}{2}\mathbf{p}_{\mathbf{u}}'\mathbf{p}_{\mathbf{u}}, \tag{5}$$

where $\mathbf{p}_{\boldsymbol{\theta}} \in \mathbb{R}^d$ and $\mathbf{p}_{\mathbf{u}} \in \mathbb{R}^D$ are the artificial momentum variables specific to $\boldsymbol{\theta}$ and $\mathbf{u}$, respectively. Note that for this form of the extended Hamiltonian the mass matrix ($\mathbf{M}$) of the compound vector $(\boldsymbol{\theta}', \mathbf{u}')'$ is selected to be block diagonal, where the mass matrix specific to $\boldsymbol{\theta}$ is denoted by $\mathbf{M}_{\boldsymbol{\theta}} \in \mathbb{R}^{d \times d}$, while the mass for $\mathbf{u}$ is set equal to the identity in order to match the precision matrix assumed for $\mathbf{u}$.

The equations of motion associated with the extended Hamiltonian (5), which obtain according to (1) for $\mathbf{q} = (\boldsymbol{\theta}', \mathbf{u}')'$ and $\mathbf{p} = (\mathbf{p}_{\boldsymbol{\theta}}', \mathbf{p}_{\mathbf{u}}')'$, are given by

$$\frac{d}{dt}\begin{pmatrix} \boldsymbol{\theta} \\ \mathbf{p}_{\boldsymbol{\theta}} \\ \mathbf{u} \\ \mathbf{p}_{\mathbf{u}} \end{pmatrix} = \begin{pmatrix} \mathbf{M}_{\boldsymbol{\theta}}^{-1}\mathbf{p}_{\boldsymbol{\theta}} \\ \nabla_{\boldsymbol{\theta}} \log p(\boldsymbol{\theta}) + \nabla_{\boldsymbol{\theta}} \log \hat{p}(\mathbf{y}|\boldsymbol{\theta}, \mathbf{u}) \\ \mathbf{p}_{\mathbf{u}} \\ -\boldsymbol{u} + \nabla_{\boldsymbol{u}} \log \hat{p}(\mathbf{y}|\boldsymbol{\theta}, \mathbf{u}) \end{pmatrix}. \tag{6}$$

6

Equation (6) shows that the Hamiltonian transition dynamics of $(\boldsymbol{\theta}, \mathbf{p}_{\boldsymbol{\theta}})$ and $(\mathbf{u}, \mathbf{p}_{\mathbf{u}})$ are linked together via their joint dependence on the MC estimate of the likelihood $\hat{p}(\mathbf{y}|\boldsymbol{\theta}, \mathbf{u})$. However, this link vanishes as the MC variance of the MC estimator $\mathrm{Var}_{\mathbf{u}}[\hat{p}(\mathbf{y}|\boldsymbol{\theta}, \mathbf{u})]$ tend to zero. In fact, an 'exact' MC estimate with zero MC variance implies that $\nabla_{\mathbf{u}} \log \hat{p}(\mathbf{y}|\boldsymbol{\theta}, \mathbf{u}) = \mathbf{0}_D$, in which case the transition dynamics of $(\boldsymbol{\theta}, \mathbf{p}_{\boldsymbol{\theta}})$ would be completely decoupled from that of $(\mathbf{u}, \mathbf{p}_{\mathbf{u}})$ and would be (marginally) the dynamics of the 'ideal' HMC for $p(\boldsymbol{\theta}|\mathbf{y})$. Moreover, the resulting marginal $(\mathbf{u}, \mathbf{p}_{\mathbf{u}})$-dynamics would reduce to that of a harmonic oscillator with analytical solutions given by $\mathbf{u}(t) = \cos(t)\mathbf{u}(0) + \sin(t)\mathbf{p}_{\mathbf{u}}(0)$ and $\mathbf{p}_{\mathbf{u}}(t) = \cos(t)\mathbf{p}_{\mathbf{u}}(0) - \sin(t)\mathbf{u}(0)$.

In order to approximate the Hamiltonian transition dynamics (6), Lindsten and Doucet (2016) develop a symplectic integrator which for exact MC likelihood estimates produces exact simulations for the dynamics of $(\mathbf{u}, \mathbf{p}_{\mathbf{u}})$ and reduces for $(\boldsymbol{\theta}, \mathbf{p}_{\boldsymbol{\theta}})$ to the conventional leap-frog integrator. They derive this integrator for the special case where the mass matrix $\mathbf{M}_{\boldsymbol{\theta}}$ in (5) and (6) is restricted to be the identity. For the more general case with an unrestricted $\mathbf{M}_{\boldsymbol{\theta}}$ this integrator for approximately advancing the dynamics from time $t = 0$ to time $t = \varepsilon$ obtains as

$$\boldsymbol{\theta}(\varepsilon/2) = \boldsymbol{\theta}(0) + (\varepsilon/2)\mathbf{M}_{\boldsymbol{\theta}}^{-1}\mathbf{p}_{\boldsymbol{\theta}}(0), \tag{7}$$

$$\mathbf{u}(\varepsilon/2) = \cos(\varepsilon/2)\mathbf{u}(0) + \sin(\varepsilon/2)\mathbf{p}_{\mathbf{u}}(0), \tag{8}$$

$$\mathbf{p}_{\mathbf{u}}^{*} = \cos(\varepsilon/2)\mathbf{p}_{\mathbf{u}}(0) - \sin(\varepsilon/2)\mathbf{u}(0), \tag{9}$$

$$\mathbf{p}_{\mathbf{u}}^{**} = \mathbf{p}_{\mathbf{u}}^{*} + \varepsilon \nabla_{\mathbf{u}}\big\{ \log \hat{p}\big[\mathbf{y} \,|\, \boldsymbol{\theta}(\varepsilon/2), \mathbf{u}(\varepsilon/2)\big] \big\}, \tag{10}$$

$$\mathbf{p}_{\boldsymbol{\theta}}(\varepsilon) = \mathbf{p}_{\boldsymbol{\theta}}(0) + \varepsilon \nabla_{\boldsymbol{\theta}}\big\{ \log p\big[\boldsymbol{\theta}(\varepsilon/2)\big] + \log \hat{p}\big[\mathbf{y} \,|\, \boldsymbol{\theta}(\varepsilon/2), \mathbf{u}(\varepsilon/2)\big] \big\}, \tag{11}$$

$$\boldsymbol{\theta}(\varepsilon) = \boldsymbol{\theta}(\varepsilon/2) + (\varepsilon/2)\mathbf{M}_{\boldsymbol{\theta}}^{-1}\mathbf{p}_{\boldsymbol{\theta}}(\varepsilon), \tag{12}$$

$$\mathbf{u}(\varepsilon) = \cos(\varepsilon/2)\mathbf{u}(\varepsilon/2) + \sin(\varepsilon/2)\mathbf{p}_{\mathbf{u}}^{**}, \tag{13}$$

$$\mathbf{p}_{\mathbf{u}}(\varepsilon) = \cos(\varepsilon/2)\mathbf{p}_{\mathbf{u}}^{**} - \sin(\varepsilon/2)\mathbf{u}(\varepsilon/2). \tag{14}$$

For producing unbiased and smoothed MC estimates of the likelihood $\hat{p}(\mathbf{y}|\boldsymbol{\theta}, \mathbf{u})$ based on standard normal auxiliary variables $\mathbf{u}$, the PM-HMC of Lindsten and Doucet (2016) relies on standard IS (see, e.g., Robert and Casella, 2004, Chap. 3.3 for a general discussion of IS). For this it is assumed that the selected IS density $m(\mathbf{x}|\boldsymbol{\theta})$ for the latent variables $\mathbf{x}$ can be simulated using a deterministic smooth function γ such that $\mathbf{x} = \gamma(\boldsymbol{\theta}, \mathbf{v})$, where $\mathbf{v} \sim N(\mathbf{0}_p, \mathbf{I}_p)$. The resulting MC-IS estimate for a given $\boldsymbol{\theta}$ then obtains by simulating $\mathbf{x}^{(i)} = \gamma(\boldsymbol{\theta}, \mathbf{v}^{(i)})$ with $\mathbf{v}^{(i)} \sim$ iid $N(\mathbf{0}_p, \mathbf{I}_p)$ for $i = 1, \ldots, n$, and computing

$$\hat{p}(\mathbf{y}|\boldsymbol{\theta}, \mathbf{u}) = \frac{1}{n}\sum_{i=1}^{n} \omega(\mathbf{x}^{(i)}), \tag{15}$$

where $\omega(\mathbf{x}^{(i)})$ denotes the IS weight given by

$$\omega(\mathbf{x}^{(i)}) = \frac{p(\mathbf{y}|\mathbf{x}^{(i)}, \boldsymbol{\theta})p(\mathbf{x}^{(i)}|\boldsymbol{\theta})}{m(\mathbf{x}^{(i)}|\boldsymbol{\theta})}, \tag{16}$$

and $\mathbf{u} = (\mathbf{v}^{(1)'}, \dots, \mathbf{v}^{(n)'})' \in \mathbb{R}^D$ with $D = np$. A natural selection for the IS density $m(\mathbf{x}|\boldsymbol{\theta})$ is the prior density $p(\mathbf{x}|\boldsymbol{\theta})$, which is the one used by Lindsten and Doucet (2016) for their applications to static hierarchical models.

2.3 PM-HMC and the Accuracy of the Likelihood Estimate

Assuming that the IS estimator $\hat{p}(\mathbf{y}|\boldsymbol{\theta}, \mathbf{u})$ in (15) is consistent in the sense that $\mathrm{Var}_{\mathbf{u}}[\hat{p}(\mathbf{y}|\boldsymbol{\theta}, \mathbf{u})] \to 0$ as $n \to \infty$, then by selecting the simulation sample size n sufficiently large the log-likelihood $\log p(\mathbf{y}|\boldsymbol{\theta})$ can be arbitrarily well approximated with a gradient of its estimate $\nabla_{\mathbf{u}} \log \hat{p}(\mathbf{y}|\boldsymbol{\theta}, \mathbf{u})$ correspondingly close to zero. Thus, for a large enough n, pseudo-marginal HMC sampling of $\boldsymbol{\theta}$ from the augmented target (4) can be made arbitrarily close to ideal HMC sampling from the exact marginal target (2). However, a strategy of increasing n typically comes at significant computational costs. First, the evaluation of $\log \hat{p}(\mathbf{y}|\boldsymbol{\theta}, \mathbf{u})$ and gradients thereof become increasingly computationally expensive. Second, an increase of n expands the dimension of the Hamiltonian system $s = d + np$, which typically necessitates a reduction of the integrator step size ε to the effect that more gradient evaluations per AR proposal for $(\boldsymbol{\theta}, \mathbf{p}_{\boldsymbol{\theta}})$ and $(\mathbf{u}, \mathbf{p}_{\mathbf{u}})$ are required. However, this second effect is relevant only up to the size of n at which $\nabla_{\mathbf{u}} \log \hat{p}(\mathbf{y}|\boldsymbol{\theta}, \mathbf{u})$ is approaching a value close to zero so that the decoupling effect for $(\boldsymbol{\theta}, \mathbf{p}_{\boldsymbol{\theta}})$ and $(\mathbf{u}, \mathbf{p}_{\mathbf{u}})$ starts dominating the Hamiltonian transition dynamics (6). (See, e.g., Beskos et al. (2013) who obtain an overall cost of HMC that is super-linear in the dimension s.)

On the other hand, a small n with non-negligible MC variation of the IS likelihood estimate (15) and values for $\nabla_{\mathbf{u}} \log \hat{p}(\mathbf{y}|\boldsymbol{\theta}, \mathbf{u})$ significantly different from zero can still result in good performance of the PM-HMC, at least as long as a critical level of accuracy for the likelihood estimate is maintained. The reason is that when $n \to 1$ the PM-HMC converges towards the standard HMC sampling on the joint space of $\boldsymbol{\theta}$ and $\mathbf{x}$ (Lindsten and Doucet, 2016). However, the class of models where standard IS ensures the required minimal accuracy of the likelihood estimate with an operational size n is fairly limited. Examples for which this is the case are the static hierarchical models with stochastically independent latent variables considered by Lindsten and Doucet (2016). For more complex latent variable models, though, the critical level of accuracy might be hard to maintain by standard IS even for a large n. For instance, in high-dimensional dynamic hierarchical models involving serially correlated latent variables standard IS like the 'brute-force' version with $m(\mathbf{x}|\boldsymbol{\theta}) = p(\mathbf{x}|\boldsymbol{\theta})$ is known to suffer for any operational size n from a 'prohibitively' large MC variance (see, e.g., Danielsson, 1994, and references therein).

From these insights into the impact of the accuracy of the likelihood estimate and the simulation sample size n on the PM-HMC, it appears to be desirable to replace standard IS by an IS procedure which (i) minimizes the MC variance for a given n so as to achieve the decoupling effect with a gradient $\nabla_{\mathbf{u}} \log \hat{p}(\mathbf{y}|\boldsymbol{\theta}, \mathbf{u})$ close to zero for a small n, and (ii) is applicable to a broad range of latent variable models. This motivates combining pseudo-marginal HMC with EIS, which is a generic IS procedure designed to achieve minimal MC variance of IS estimates for (potentially high-dimensional) likelihood integrals.

3 PM-HMC with EIS

3.1 EIS Principle

In order to minimize the variance of IS estimates for the likelihood of non-Gaussian and/or non-linear latent variable models as given in (3), EIS aims at sequentially constructing an IS density which approximates, as close as possible, the (infeasible) optimal IS density $m^*(\mathbf{x}|\boldsymbol{\theta}) \propto p(\mathbf{y}|\mathbf{x}, \boldsymbol{\theta}) p(\mathbf{x}|\boldsymbol{\theta})$, which would reduce the variance of likelihood estimates to zero.

With reference to the likelihood (3) it is assumed that the conditional data density $p(\mathbf{y}|\mathbf{x}, \boldsymbol{\theta})$ and the prior for the latent variables $p(\mathbf{x}|\boldsymbol{\theta})$ under the latent variable model can be factorized as functions in $\mathbf{x} = (x_1, \ldots, x_T)$ into

$$p(\mathbf{y}|\mathbf{x}, \boldsymbol{\theta}) = \prod_{t=1}^{T} g_t(x_t, \boldsymbol{\delta}), \qquad p(\mathbf{x}|\boldsymbol{\theta}) = \prod_{t=1}^{T} f_t(x_t|\mathbf{x}_{(t-1)}, \boldsymbol{\delta}), \tag{17}$$

where $\mathbf{x}_{(t)} = (x_1, \ldots, x_t)$ with $\mathbf{x}_{(T)} = \mathbf{x}$ and $\boldsymbol{\delta} = (\boldsymbol{\theta}, \mathbf{y})$. Such factorizations can be found for a broad class of models, including dynamic non-Gaussian/non-linear SSMs for time series, non-Gaussian/non-linear models with a latent correlation structure for cross-sectional data as well as static hierarchical models without latent correlation for which $f_t(x_t|\mathbf{x}_{(t-1)}, \boldsymbol{\delta}) = f_t(x_t, \boldsymbol{\delta})$. In our applications below we consider univariate time series models, which is why we use t to index the elements in $\mathbf{x}$ and restrict x_t in (17) to be one-dimensional.

EIS-MC estimation of likelihood functions of the form (3) and (17) is based upon an IS density m for $\mathbf{x}$ which is decomposed conformably with the factorization in (17) into

$$m(\mathbf{x}|\mathbf{a}) = \prod_{t=1}^{T} m_t(x_t|\mathbf{x}_{(t-1)}, \mathbf{a}_t), \tag{18}$$

9

with conditional densities m_t such that

$$m_t(x_t|\mathbf{x}_{(t-1)}, \mathbf{a}_t) = \frac{k_t(\mathbf{x}_{(t)}, \mathbf{a}_t)}{\chi_t(\mathbf{x}_{(t-1)}, \mathbf{a}_t)}, \quad \chi_t(\mathbf{x}_{(t-1)}, \mathbf{a}_t) = \int k_t(\mathbf{x}_{(t)}, \mathbf{a}_t)dx_t, \tag{19}$$

where $\mathcal{K} = \{k_t(\cdot, \mathbf{a}_t), \mathbf{a}_t \in \mathcal{A}_t\}$ is a preselected parametric class of density kernels indexed by auxiliary parameters $\mathbf{a}_t$ and with a point-wise computable integrating factor χ_t. As required for PM-HMC it is assumed that the IS density (18) can be simulated by sequentially generating draws from the conditional densities (19) using smooth deterministic functions γ_t such that $x_t = \gamma_t(\mathbf{a}_t, v_t)$ for $t = 1, \ldots, T$, where $v_t \sim N(0, 1)$.

From (17)-(19) results the following factorized IS representation of the likelihood (3):

$$p(\mathbf{y}|\boldsymbol{\theta}) = \int \left[\prod_{t=1}^{T} \omega_t(\mathbf{x}_{(t)}, \mathbf{a}_{(t+1)}) \right] m(\mathbf{x}|\mathbf{a})d\mathbf{x}, \tag{20}$$

where the period-t IS weight is given by

$$\omega_t(\mathbf{x}_{(t)}, \mathbf{a}_{(t+1)}) = \frac{g_t(x_t, \boldsymbol{\delta})f_t(x_t|\mathbf{x}_{(t-1)}, \boldsymbol{\delta})\chi_{t+1}(\mathbf{x}_{(t)}, \mathbf{a}_{t+1})}{k_t(\mathbf{x}_{(t)}, \mathbf{a}_t)}, \tag{21}$$

with $\chi_{T+1}(\cdot) \equiv 1$. For any given $\mathbf{a} = (\mathbf{a}_1, \ldots, \mathbf{a}_T) \in \mathcal{A} = \times_{t=1}^{T} \mathcal{A}_t$, the corresponding MC likelihood estimate obtains as

$$\hat{p}(\mathbf{y}|\boldsymbol{\theta}, \mathbf{u}) = \frac{1}{n}\sum_{i=1}^{n} \omega(\mathbf{x}^{(i)}, \mathbf{a}), \qquad \omega(\mathbf{x}^{(i)}, \mathbf{a}) = \prod_{t=1}^{T} \omega_t(\mathbf{x}_{(t)}^{(i)}, \mathbf{a}_{(t+1)}), \tag{22}$$

where $\{\mathbf{x}^{(i)}\}_{i=1}^{n}$ are n iid draws simulated from the sequential IS density $m(\mathbf{x}|\mathbf{a})$ in (18), and $\mathbf{u} = (\mathbf{v}^{(1)'}, \ldots, \mathbf{v}^{(n)'})'$ with $\mathbf{v}^{(i)} = (v_1^{(i)}, \ldots, v_T^{(i)})' \sim$ iid $N(\mathbf{0}_T, \mathbf{I}_T)$ for $i = 1, \ldots, n$, so that the dimension of $\mathbf{u}$ is $D = nT$.

In order to minimize the MC variance of the likelihood estimate (22), EIS aims at selecting values for the auxiliary parameters $\mathbf{a}$ that minimize period-by-period the MC variance of the IS weights ω_t in (21) with respect to $m(\mathbf{x}|\mathbf{a})$. This requires that the kernels $k_t(\mathbf{x}_{(t)}, \mathbf{a}_t)$ as functions in $\mathbf{x}_{(t)}$ provide the best possible fit to the products $g_t(x_t, \boldsymbol{\delta})f_t(x_t|\mathbf{x}_{(t-1)}, \boldsymbol{\delta})\chi_{t+1}(\mathbf{x}_{(t)}, \mathbf{a}_{t+1})$. For an approximate solution to this minimization problem under the preselected class of kernels $\mathcal{K}$, EIS solves the following back-recursive sequence of least

squares (LS) approximation problems:

$$(\hat{c}_t, \hat{\mathbf{a}}_t) = \arg\min_{\mathbf{a}_t \in \mathcal{A}_t, \alpha_t \in \mathbb{R}} \sum_{i=1}^{r} \left\{ \log\left[g_t\big(x_t^{(i)}, \boldsymbol{\delta}\big) \ f_t\big(x_t^{(i)}|\mathbf{x}_{(t-1)}^{(i)}, \boldsymbol{\delta}\big) \ \chi_{t+1}\big(\mathbf{x}_{(t)}^{(i)}, \hat{\mathbf{a}}_{t+1}\big) \right] \right.$$
$$\left. - c_t - \log k_t\big(\mathbf{x}_{(t)}^{(i)}, \mathbf{a}_t\big) \right\}^2, \qquad t = T, T-1, \ldots, 1, \tag{23}$$

where c_t represents an intercept, and $\{\mathbf{x}^{(i)}\}_{i=1}^{r}$ denote r iid draws simulated from $m(\mathbf{x}|\mathbf{a})$ itself. Thus, the EIS-optimal values for the auxiliary parameters $\hat{\mathbf{a}}$ result as a fixed-point solution to the sequence $\{\hat{\mathbf{a}}^{[0]}, \hat{\mathbf{a}}^{[1]}, \ldots\}$ in which $\hat{\mathbf{a}}^{[j]}$ is obtained from (23) under draws from $m(\mathbf{x}|\hat{\mathbf{a}}^{[j-1]})$. In order to ensure convergence to a fixed-point solution it is critical that all the $\mathbf{x}$ draws simulated for the sequence $\{\hat{\mathbf{a}}^{[j]}\}$ be generated by using the smooth deterministic functions γ_t to transform a *single set* of rT Common Random Numbers (CRNs), say $\mathbf{z} \sim N(\mathbf{0}_{rT}, \mathbf{I}_{rT})$. To initialize the fixed-point iterations $j = 0, \ldots, J$, the starting value $\hat{\mathbf{a}}^{[0]}$ can be obtained, e.g., from an analytical local approximation (such as Laplace) of the EIS targets $\ln(g_t f_t \chi_{t+1})$ in (23). Convergence of the iterations to a fixed-point solution is typically fast to the effect that a value for the number of iterations J between 2 and 4 often suffices to produce a (close to) optimal solution (Richard and Zhang, 2007). The MC-EIS likelihood estimate for a given $\boldsymbol{\theta}$ then obtains by substituting in (22) the EIS-optimal value $\hat{\mathbf{a}}$ for $\mathbf{a}$. In order to highlight its dependence on $\boldsymbol{\theta}$ and $\mathbf{z}$ we shall use $\hat{\mathbf{a}} = \mathbf{a}(\boldsymbol{\theta}, \mathbf{z})$ to denote the EIS-optimal value.

The selection of the parametric class $\mathcal{K}$ of EIS density kernels k_t is inherently specific to the latent variable model under consideration as those kernels are meant to provide a functional approximation in $\mathbf{x}_{(t)}$ to the product $g_t f_t \chi_{t+1}$. In the applications below, we consider models with data densities g_t which are log-concave in x_t and Gaussian conditional densities for x_t with a Markovian structure so that $f_t(x_t|\mathbf{x}_{(t-1)}, \boldsymbol{\delta}) = f_t(x_t|x_{t-1}, \boldsymbol{\delta})$. This suggests to select the k_t's as Gaussian kernels and to exploit that such kernels are closed under multiplication in order to construct the k_t's as the following parametric extensions of the prior densities f_t:

$$k_t(x_t, x_{t-1}, \mathbf{a}_t) = f_t(x_t|x_{t-1}, \boldsymbol{\delta})\xi_t(x_t, \mathbf{a}_t), \tag{24}$$

where ξ_t is a Gaussian kernel in x_t of the form $\xi_t(x_t, \mathbf{a}_t) = \exp\{a_{1t}x_t + a_{2t}x_t^2\}$ with $\mathbf{a}_t = (a_{1t}, a_{2t})$. In this case the EIS approximation problems (23) take the form of simple *linear* LS-problems where $\log[g_t(x_t^{(i)}, \boldsymbol{\delta})$ $\chi_{t+1}(x_t^{(i)}, \hat{\mathbf{a}}_{t+1})]$ are regressed on a constant, $x_t^{(i)}$ and $[x_t^{(i)}]^2$. Such linear LS regressions for (23), which simplify EIS implementations, obtain for all kernels k_t chosen within the exponential family (Richard and Zhang, 2007). However, it is important to note that EIS is by no means restricted to the use of IS densities from

11

the exponential family nor to models with low-order Markovian specifications for the latent variables. EIS implementations with more flexible IS densities such as mixture of normal distributions are found in Kleppe and Liesenfeld (2014), Scharth and Kohn (2016), Grothe et al. (2018), and Liesenfeld and Richard (2010) use truncated normal distributions. Applications of EIS to models with non-Markovian latent variables for spatial data are provided in Liesenfeld et al. (2016, 2017).

The EIS approach as outlined above differs from standard IS in that it uses IS densities whose parameters $\hat{\mathbf{a}} = \mathbf{a}(\boldsymbol{\theta}, \mathbf{z})$ are (conditional on $\boldsymbol{\theta}$) random variables as they depend via the EIS fixed-point repressions (23) on the CRNs $\mathbf{z}$. This calls for specific rules for implementing EIS which ensure that the resulting MC likelihood estimates meet the qualifications needed for their use within PM-HMC. In order to ensure that the EIS likelihood estimate (22) based on the random numbers $\mathbf{u}$ is unbiased the latter need to be a set of random draws different from the CRNs $\mathbf{z}$ used to find $\hat{\mathbf{a}}$ (Kleppe and Liesenfeld, 2014). Note also that since $\hat{\mathbf{a}}$ is an implicit function of $\boldsymbol{\theta}$, maximal accuracy requires us to rerun the EIS fixed-point regressions for any new value of $\boldsymbol{\theta}$. In order to ensure that the resulting EIS likelihood estimate (22) as a function of $\hat{\mathbf{a}}$ is smooth in $\boldsymbol{\theta}$, $\hat{\mathbf{a}}$ itself needs to be a smooth function of $\boldsymbol{\theta}$. This can be achieved by presetting the number of fixed-point iterations J across all $\boldsymbol{\theta}$-values to a fixed number, rather than using a stopping rule based on a relative-change threshold.

3.2   The PM-HMC-EIS Algorithm

Since EIS provides unbiased MC likelihood estimates $\hat{p}(\mathbf{y}|\boldsymbol{\theta}, \mathbf{u})$ which can be obtained as a smooth function of the parameters $\boldsymbol{\theta}$ and auxiliary standard normal random numbers $\mathbf{u}$, we propose to combine it with the PM-HMC approach in Section 2.2. As discussed above, EIS offers the possibility to substantially reduce the MC variance relative to standard IS so that the resulting PM-HMC can be expected to closely approximate the ideal marginal HMC with decoupled transition dynamics for $(\boldsymbol{\theta}, \mathbf{p}_{\boldsymbol{\theta}})$ and $(\mathbf{u}, \mathbf{p_u})$ even for a small simulation sample size n.

The validity of this PM-HMC algorithm based on EIS, however, requires to account for the randomness of the optimal EIS parameters $\hat{\mathbf{a}} = \mathbf{a}(\boldsymbol{\theta}, \mathbf{z})$ indexing the IS density $m(\mathbf{x}|\hat{\mathbf{a}})$ used for likelihood estimation. In order to account for this randomness the CRNs $\mathbf{z}$ used to obtain $\hat{\mathbf{a}}$ need to be included into the Markov kernel of the PM-HMC so that it leaves the target posterior $p(\boldsymbol{\theta}|\mathbf{y})$ invariant. This can be easily achieved by drawing in each PM-HMC sweep k a new set of CRNs $\mathbf{z}^{(k)}$ (Kleppe, 2017; Grothe et al., 2018).

A full description of the resulting PM-HMC-EIS is provided in Algorithm 1. The selection of the HMC- and EIS-specific tuning parameters for the algorithm as well as operational details are discussed in the next section.

Algorithm 1 PM-HMC with EIS targeting $p(\boldsymbol{\theta}|\mathbf{y}) \propto p(\mathbf{y}|\boldsymbol{\theta})p(\boldsymbol{\theta})$.

1: Input: n, r, J, N, L, ε.

2: Simulate EIS CRNs $\mathbf{z}$ and $\mathbf{u}$: $\mathbf{z}^{(*)} \sim N(\mathbf{0}_{rT}, \mathbf{I}_{rT})$ and $\mathbf{u}^{(*)} \sim N(\mathbf{0}_{nT}, \mathbf{I}_{nT})$.

3: Use EIS likelihood estimation (22) based on $\mathbf{u}^{(*)}$ and EIS parameters $\hat{\mathbf{a}} = \mathbf{a}(\boldsymbol{\theta}, \mathbf{z}^{(*)})$ to obtain the simulated MAP value: $\hat{\boldsymbol{\theta}} = \arg\max_{\boldsymbol{\theta}} \log\left[\hat{p}(\mathbf{y}|\boldsymbol{\theta}, \mathbf{u}^{(*)})p(\boldsymbol{\theta})\right]$.

4: Set $\mathbf{M}_{\boldsymbol{\theta}} = -\nabla_{\boldsymbol{\theta}}^2 \log\left[\hat{p}(\mathbf{y}|\boldsymbol{\theta}, \mathbf{u}^{(*)})p(\boldsymbol{\theta})\right]\big|_{\boldsymbol{\theta}=\hat{\boldsymbol{\theta}}}$.

5: Simulate initial values for $\boldsymbol{\theta}$ and $\mathbf{u}$: $\boldsymbol{\theta}^{(0)} \sim N(\hat{\boldsymbol{\theta}}, \mathbf{M}_{\boldsymbol{\theta}}^{-1})$, $\mathbf{u}^{(0)} \sim N(\mathbf{0}_{nT}, \mathbf{I}_{nT})$.

6: **for** $1 \leq k \leq N$ **do**

7:      Refresh momentums: $\mathbf{p}_{\boldsymbol{\theta}}(0) \sim N(\mathbf{0}_d, \mathbf{M}_{\boldsymbol{\theta}})$ and $\mathbf{p}_{\mathbf{u}}(0) \sim N(\mathbf{0}_{nT}, \mathbf{I}_{nT})$.

8:      Set $\boldsymbol{\theta}(0) = \boldsymbol{\theta}^{(k-1)}$ and $\mathbf{u}(0) = \mathbf{u}^{(k-1)}$.

9:      Simulate EIS CRNs $\mathbf{z}$: $\mathbf{z}^{(k)} \sim N(\mathbf{0}_{rT}, \mathbf{I}_{rT})$.

10:      Use (7)-(14) to advance dynamics from $[\boldsymbol{\theta}(0), \mathbf{p}_{\boldsymbol{\theta}}(0), \mathbf{u}(0), \mathbf{p}_{\mathbf{u}}(0)]$ to $[\boldsymbol{\theta}(L\varepsilon), \mathbf{p}_{\boldsymbol{\theta}}(L\varepsilon), \mathbf{u}(L\varepsilon), \mathbf{p}_{\mathbf{u}}(L\varepsilon)]$ by performing L integrator steps $\ell = \varepsilon, 2\varepsilon, \ldots, L\varepsilon$ with step size ε and using EIS likelihood estimation (22) based on $\mathbf{u}(\ell)$ and EIS parameters $\hat{\mathbf{a}} = \mathbf{a}(\boldsymbol{\theta}(\ell), \mathbf{z}^{(k)})$.

11:      **if** $\mathcal{U}(0,1) < \min\{1, \exp(H[\boldsymbol{\theta}(0), \mathbf{p}_{\boldsymbol{\theta}}(0), \mathbf{u}(0), \mathbf{p}_{\mathbf{u}}(0)] - H[\boldsymbol{\theta}(L\varepsilon), \mathbf{p}_{\boldsymbol{\theta}}(L\varepsilon), \mathbf{u}(L\varepsilon), \mathbf{p}_{\mathbf{u}}(L\varepsilon)])\}$ **then**

12:          $\boldsymbol{\theta}^{(k)} = \boldsymbol{\theta}(L\varepsilon)$, $\mathbf{u}^{(k)} = \mathbf{u}(L\varepsilon)$

13:      **else**

14:          $\boldsymbol{\theta}^{(k)} = \boldsymbol{\theta}^{(k-1)}$, $\mathbf{u}^{(k)} = \mathbf{u}^{(k-1)}$

15:      **end if**

16: **end for**

17: **return** $\{\boldsymbol{\theta}^{(k)}\}_{k=1}^N$.

3.3 Tuning Parameters and Operational Details

The HMC specific tuning parameters to be selected are the mass matrix $\mathbf{M}_{\boldsymbol{\theta}}$ in the extended Hamiltonian (4) and the step size ε together with the number of steps L for the numerical integrator in (7)-(14). Since in our applications below the shape of the posteriors $p(\boldsymbol{\theta}|\mathbf{y})$ is expected to be not too different from that of a Gaussian distribution and the PM-HMC-EIS aims at getting close to a decoupled HMC transition dynamics for $(\boldsymbol{\theta}, \mathbf{p}_{\boldsymbol{\theta}})$ and $(\mathbf{u}, \mathbf{p}_{\mathbf{u}})$ in (6), we can follow for this selection the general guidelines for tuning a standard HMC targeting a (close to) Gaussian posterior.

According to those guidelines, the $\mathbf{M}_{\boldsymbol{\theta}}$ should be set close to the precision matrix of $p(\boldsymbol{\theta}|\mathbf{y})$ (Neal, 2011). This suggests to use for $\mathbf{M}_{\boldsymbol{\theta}}$ an EIS estimate for the precision matrix of the posterior $-\nabla_{\boldsymbol{\theta}}^2 \log\left[\hat{p}(\mathbf{y}|\boldsymbol{\theta}, \mathbf{u})p(\boldsymbol{\theta})\right]$, evaluated at the EIS simulated MAP value $\hat{\boldsymbol{\theta}} = \arg\max_{\boldsymbol{\theta}} \log\left[\hat{p}(\mathbf{y}|\boldsymbol{\theta}, \mathbf{u})p(\boldsymbol{\theta})\right]$.

In order to ensure continuity of the EIS likelihood estimate with respect to $\boldsymbol{\theta}$ which is critical for the MAP maximization, the EIS fixed-point regressions need to be run for each new $\boldsymbol{\theta}$ value with the same set of CRNs $\mathbf{z}$ and the corresponding likelihood estimates have to be obtained from the same set of auxiliary random numbers $\mathbf{u}$. As for the integrator step size ε and the corresponding number of steps L, we select

their values such that the total (artificial) integration time εL is approximately equal to $\pi/2$ and then tune $\varepsilon = \pi/(2L)$ such that the acceptance probability for the AR-proposals of $(\boldsymbol{\theta}, \mathbf{p_\theta}, \mathbf{u}, \mathbf{p_u})$ is close to 0.9 (Neal, 2011; Mannseth et al., 2018).

The EIS-specific tuning parameters are the number of $\mathbf{x}^{(i)}$-draws r used to run the EIS regressions (23), the number of fixed-point iterations on the EIS regressions J, and the number of $\mathbf{x}^{(i)}$-draws n for the likelihood estimate (22). Those parameters should be selected so as to balance the trade-off between EIS computing time and the quality of the resulting EIS density with respect to the MC accuracy. In particular, for r it is recommended to select it as small as possible while retaining the EIS fixed-point regressions numerically stable and the parameter J should be set such that it is guaranteed that the fixed-point sequence $\{\mathbf{a}^{[j]}\}_j$ approximately converge for the $\boldsymbol{\theta}$ values in the relevant range of the parameter space. In our application below, where the selected class of kernels $\mathcal{K}$ imply that the EIS regressions are linear in the EIS parameters $\mathbf{a}_t$ we find that a J set equal to 1 or 2 and an r about 2 times the number of parameters in $(\mathbf{a}_t, c_t)$ suffice to obtain EIS kernels k_t providing highly accurate approximations to the targeted product $g_t f_t \chi_{t+1}$ with an R^2 of the EIS regressions in the final iteration typically larger than 0.95. Finally, the optimal value for n depends on the level of accuracy of that approximation and it should be selected such that the joint HMC-dynamics in (6) is close to be decoupled while keeping computing costs and the dimension of the Hamiltonian system $s = d + nT$ as low as possible. In our applications we find $n = 1$ to be optimal reflecting the fact that the EIS densities provide highly accurate likelihood estimates.

The bulk of computing time for running Algorithm 1 is required for computing the gradients of the EIS likelihood estimates with respect to $\boldsymbol{\theta}$ and $\mathbf{u}$ in the numerical integrator (see update equations 10 and 11). The gradient with respect to $\boldsymbol{\theta}$ is also required for the MAP maximization and computation of the Hessian used for the tuning parameter $\mathbf{M_\theta}$. In order to obtain those gradients in an exact form we rely on Automatic Differentiation (AD) (see, e.g., Griewank, 2000), and use for its implementation the Adept C++ automatic differentiation software library (Hogan, 2014). With respect to computation time for AD gradient evaluations it bears mentioning the so-called 'cheap gradient principle' of backward mode automatic differentiation which states that the calculation of a gradient is only proportional to the computational complexity of the algorithm being differentiated, regardless of the number of input variables (Griewank, 2000). This implies for our application that the computational costs for computing AD gradients grows only linearly with n.

4 Applications

In this section we present applications of the PM-HMC-EIS to three dynamic non-Gaussian/non-linear latent variable models. The specific models are selected to illustrate the performance of PM-HMC-EIS under different empirically relevant scenarios. The PM-HMC-EIS algorithm is implemented using the R package Rcpp by Eddelbuettel and François (2011), which makes it possible to run compiled C++ code in R (R Core Team, 2018). All computations are performed using multi-core support for R version 3.4.3 on a 2016 iMac with a 3.1GHz Intel Core i5 processor.

For comparison, we implement as a benchmark standard HMC for sampling on the joint space of the parameters and latent variables. For this we use Stan, which is a programming language providing automatic routines for the no-U-turn sampler of Hoffman and Gelman (2014) and for HMC parameter tuning based on a dual averaging scheme (Stan Development Team, 2017). The Stan-HMC sampler is implemented by taking the canonical innovations of the latent x_t-processes as the target variables to be simulated rather than the x_t's themselves. As the scale of those innovations (given by η_t in the model descriptions below) does not depend on the model parameters this Stan-HMC implementation performs typically better than that using the x_t's as target variables (see, e.g., Stan Development Team, 2017, chapter 10.5). Stan is used through its R interface rstan (Stan Development Team, 2018), version 2.17.3.

For each of the three model applications the PM-HMC-EIS is simulated for 1,500 iterations, where the draws from the first 500 burn-in iterations are discarded. As sampling on the joint space of $\boldsymbol{\theta}$ and $\boldsymbol{\eta} = (\eta_1, \ldots, \eta_T)'$ can be expected to require more iterations to get into the stationary region Stan-HMC is simulated for 2,000 iterations with 1,000 burn-in steps.

4.1 Stochastic Volatility Model

The first example model is the discrete-time stochastic volatility (SV) model for financial returns given by (Taylor, 1986)

$$y_t = \exp(x_t/2)e_t, \quad e_t \sim \text{iid } N(0,1) \tag{25}$$

$$x_t = \gamma + \delta x_{t-1} + \nu \eta_t, \quad \eta_t \sim \text{iid } N(0,1), \tag{26}$$

where y_t is the return observed on day t, x_t is the latent log-volatility with initial condition $x_1 \sim N(\gamma/[1 - \delta], \nu^2/[1 - \delta^2])$, while e_t and η_t are mutually independent innovations. The data we use for the SV model consists of daily log-returns on the U.S. dollar against the U.K. Pound Sterling from October 1, 1981 to June 28, 1985 with $T = 945$. A description of this classical data set is found in Harvey et al. (1994). The
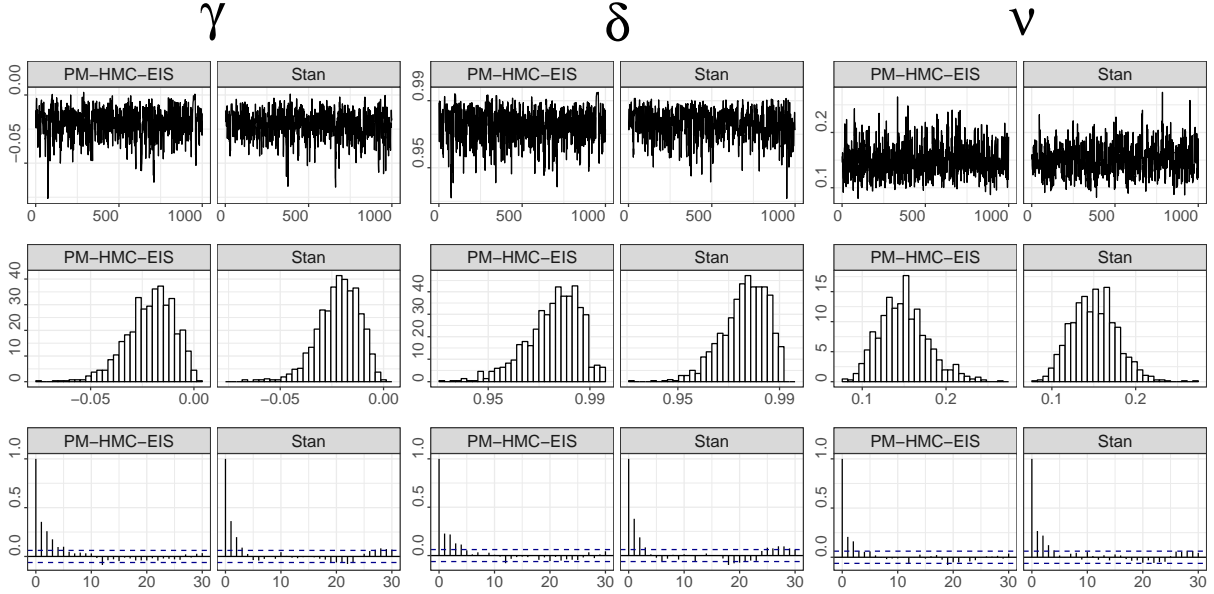
Figure 1: Trace plots (top), histograms (middle) and empirical autocorrelation functions (bottom) for a representative replica of PM-HMC-EIS and Stan-HMC applied to the SV model in (25) and (26) for the Dollar/Pound exchange rate data.

standard prior assumptions for the parameters $\boldsymbol{\theta} = (\gamma, \delta, \nu)$ are the following: for γ we use a flat prior, for $(\delta + 1)/2$ a Beta prior $\mathcal{B}(\alpha, \beta)$ with $\alpha = 20$ and $\beta = 1.5$, and for ν^2 a scaled inverted-χ^2 prior $p_0 s_0 / \chi^2_{(p_0)}$ with $p_0 = 10$ and $s_0 = 0.01$. For numerical stability we use the parametrization $\boldsymbol{\theta}^* = (\gamma, \text{arctanh} \, \delta, \log \nu^2)$ together with the priors for $\boldsymbol{\theta}^*$ as obtained from those on $\boldsymbol{\theta}$ to run the HMC algorithms.

Under this SV model the data density $g_t(x_t, \boldsymbol{\delta}) = \mathcal{N}(y_t | 0, \exp\{x_t\})$ is fairly uninformative about the states x_t and their innovations η_t with a Fisher information which is independent of $\boldsymbol{\theta}$ and given by $-E[\nabla^2_{x_t} \log g_t(x_t, \boldsymbol{\delta})] = 1/2$, whereas the states are fairly volatile under typical estimates for $\boldsymbol{\theta}$. This low signal-to-noise ratio together with a shape of the data density which is independent of the parameters implies that the conditional posterior of the innovations $\boldsymbol{\eta}$ given $\boldsymbol{\theta}$ are close to a normal distribution regardless of $\boldsymbol{\theta}$, leading to a correspondingly well-behaved joint posterior of $\boldsymbol{\theta}$ and $\boldsymbol{\eta}$. Hence, this represents a scenario where the Stan-HMC sampling on the joint space of $\boldsymbol{\theta}$ and $\boldsymbol{\eta}$ used as a benchmark can be expected to exhibit a comparably good performance.

The PM-HMC-EIS for this model is implemented with $J = 2$ EIS fixed-point iterations for a CRN sample size of $r = 6$. This proved to be sufficient to obtain EIS densities producing highly accurate likelihood estimates so that the simulation sample size for those estimates can be selected to be as low as $n = 1$. For the remaining tuning parameters we use $\varepsilon = 0.4$ and $L = 4$. In Figure 1 we display the trace plots, histograms and autocorrelation functions (ACF) for the parameters simulated from the posterior using PM-HMC-EIS and Stan-HMC. From the results we see that both procedures are performing similarly well in exploring

		PM-HMC-EIS		Stan-HMC	
		Min	Mean	Min	Mean
	CPU time (s)	193.4	254.8	9.2	11.7
	Acc. rate	0.88	0.90	0.82	0.89
γ	Post. mean		-0.0212		-0.0215
	Post. std.		0.0116		0.0108
	ESS	264.8	362.0	246.3	395.6
	ESS/s	0.54	1.57	26.50	35.06
δ	Post. mean		0.9757		0.9763
	Post. std.		0.0106		0.0094
	ESS	328.3	396.2	222.1	380.5
	ESS/s	0.67	1.70	23.90	34.49
ν	Post. mean		0.1497		0.1524
	Post. std.		0.0293		0.0278
	ESS	436.0	495.1	234.5	369.3
	ESS/s	1.07	2.08	23.64	33.37

Table 1: Posterior mean and standard deviation, ESS, ESS/s, and acceptance probability of PM-HMC-EIS and Stan-HMC samples of size $N = 1,000$ for the parameters of the SV model in (25) and (26) applied to the Dollar/Pound exchange rate data. The columns 'Min' and 'Mean' correspond to the minimum and mean across 8 independent replica of the experiment. Burn-in iterations are not included in the reported CPU times.
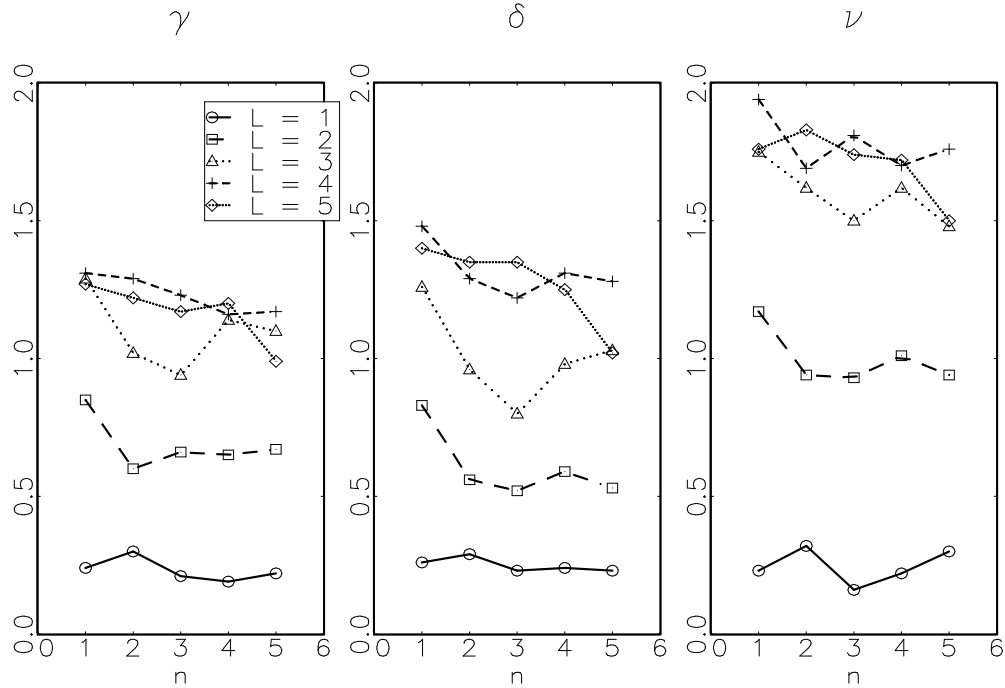

Figure 2: ESS/s values of posterior PM-HMC-EIS samples for the parameters of the SV model in (25) and (26) applied to the Dollar/Pound exchange rate data. ESS/s values are plotted as functions of the simulation sample size n for different numbers of steps L used in the numerical integrator. The plotted ESS/s values are the mean across 8 independent runs of the PM-HMC-EIS for $N = 10,000$ iterations.

17

the target distribution. The ACF plots indicate that Stan-HMC as well as PM-HMC-EIS produce samples which are fairly close to be iid draws from the posterior. This mixing of PM-HMC-EIS and Stan-HMC for the SV parameters is much faster than that typically observed for Gibbs procedures alternately updating the parameters and the latent volatility states (see, e.g., Bos and Shephard, 2006; Grothe et al., 2018) and of pseudo marginal methods updating the SV parameter using standard Metropolis Hasting schemes (see, e.g., Flury and Shephard, 2011).

Table 1 shows the HMC posterior mean and standard deviation for the parameters, which are sample averages computed from 8 independent replications obtained by running the HMC algorithms under 8 different seeds. It also reports the effective sample size (ESS) of the posterior samples defined as $N\left[1 + 2\sum_{w=1}^{W}\gamma(w)\right]^{-1}$, where N denotes the size of the posterior sample, and $\sum_w \gamma(w)$ aggregates the W monotone sample autocorrelations (Geyer, 1992). ESS is the accuracy equivalent for the actual sample of size N in terms of the size of an hypothetical iid sample from the posterior. The reported ESS figures are the average and minimum across the 8 replications and their standardized counterparts obtained by normalizing the ESS by the Central Processor Unit (CPU) time in seconds required to run the HMC algorithms (ESS/s). The ESS results in Table 1 indicate that the PM-HMC-EIS mixes slightly faster than Stan-HMC. However, due to its comparably very low computing time, the latter produces a larger effective sample for $\boldsymbol{\theta}$ per second computing time.

In order to analyze the sensitivity of the performance of the PM-HMC-EIS with respect to the simulation sample size n used for EIS likelihood estimation and the number of HMC integrator steps L we plot in Figure 2 the mean of ESS/s for the SV parameters across 8 independent replications for a range of different values for n and L. They are obtained from running the PM-HMC-EIS in each replication for 10,000 iterations after 500 burn-in steps using $J = 2$ and $r = 6$. The plotted ESS/s values clearly indicate that the balance between the quality of the MCMC sample and computing time achieved by PM-HMC-EIS with $n = 1$ together with $L = 4$ does not improve by increasing n and adjusting L.

4.2 Gamma Model for Realized Volatilities

The second example model is a dynamic SSM for the realized variance of asset returns (see, e.g., Golosnoy et al., 2012, and references therein). It has the form

$$y_t = \beta \exp(x_t)e_t, \quad e_t \sim \text{iid } G(1/\tau, \tau) \tag{27}$$

$$x_t = \delta x_{t-1} + \nu \eta_t, \quad \eta_t \sim \text{iid } N(0, 1), \tag{28}$$
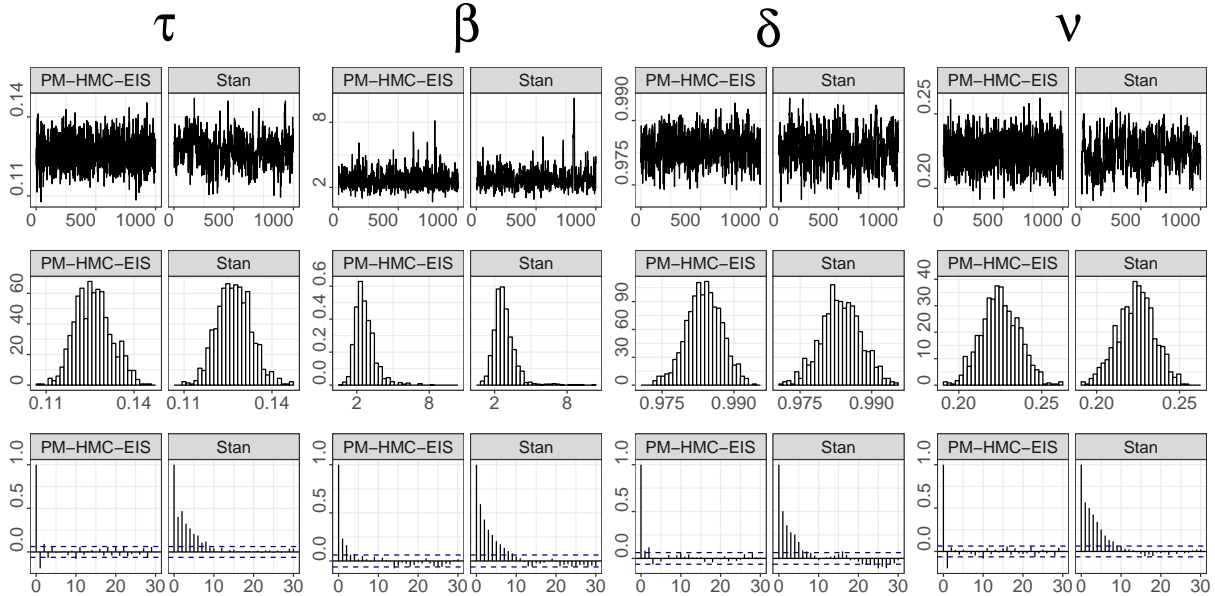
Figure 3: Trace plots (top), histograms (middle) and empirical autocorrelation functions (bottom) for a representative replica of PM-HMC-EIS and Stan-HMC applied to the Gamma model in (27) and (28) for the American Express realized volatilities data.

where y_t is the daily realized variance measuring the latent integrated variance $\beta \exp(x_t)$, and $G(1/\tau, \tau)$ denotes a Gamma-distribution for e_t normalized such that $E(e_t) = 1$ and $\text{Var}(e_t) = \tau$. The innovations e_t and η_t are independent and the initial condition for the log-variance is $x_1 \sim N(0, \nu^2/[1 - \delta^2])$. This Gamma volatility model is applied to a data set consisting of $T = 2,514$ observations of the daily realized variance for the American Express stock with a sample period ranging from January 1, 2000 to December 31, 2009. Details about this data set are found in Golosnoy et al. (2012). As for the priors on the parameters $\boldsymbol{\theta} = (\tau, \beta, \delta, \nu)$, we assume that they are flat for $\log \tau$ as well as $\log \beta$, a Beta $\mathcal{B}(\alpha, \beta)$ with $\alpha = 20$ and $\beta = 1.5$ for $(\delta + 1)/2$, and a scaled inverted-χ^2 for ν^2 with $p_0 s_0/\chi^2_{(p_0)}$ and $p_0 = 10$, $s_0 = 0.01$. For the HMC computations we use the parameterization $\boldsymbol{\theta}^* = (\log \tau, \log \beta, \text{arctanh}\, \delta, \log \nu^2)$.

In contrast to the SV model, this Gamma model applied to the realized variance data has both a considerably higher signal-to-noise ratio and a shape of the data density $g_t(x_t, \boldsymbol{\delta})$ which depends on the parameters. In particular, the Fisher information of its data density with respect to x_t is $1/\tau$ with an estimate of $\tau \simeq 0.13$ (see Table 2), while the estimated volatility of the states is roughly as large as under the SV model. Hence, it can be expected that the conditional posterior of the innovations $\boldsymbol{\eta}$ given $\boldsymbol{\theta}$ deviates distinctly from a Gaussian form and exhibits nonlinear dependence on $\boldsymbol{\theta}$, which makes the Gamma model a more challenging scenario for the Stan-HMC benchmark than the SV model.

Similar to the SV model, $J = 2$ EIS iterations for a CRN sample size $r = 5$ provide highly efficient EIS densities so that we can set the simulation sample size for the EIS likelihood estimation to $n = 1$. For the

		PM-HMC-EIS		Stan-HMC	
		Min	Mean	Min	Mean
	CPU time (s)	738.6	742.0	125.2	161.5
	Acc. rate	0.85	0.87	0.88	0.91
τ	Post. mean		0.1263		0.1270
	Post. std.		0.0060		0.0058
	ESS	1000	1000	166.3	222.6
	ESS/s	1.34	1.35	0.92	1.45
β	Post. mean		2.6567		2.8597
	Post. std.		0.8355		1.0618
	ESS	294.2	519.7	47.7	268.7
	ESS/s	0.39	0.70	0.37	1.60
δ	Post. mean		0.9838		0.9838
	Post. std.		0.0039		0.0039
	ESS	496.2	650.9	140.6	291.6
	ESS/s	0.67	0.88	1.09	1.86
ν	Post. mean		0.2248		0.2240
	Post. std.		0.0111		0.0108
	ESS	768.5	971.1	117.2	166.1
	ESS/s	1.03	1.31	0.63	1.09

Table 2: Posterior mean and standard deviation, ESS, ESS/s, and acceptance probability of PM-HMC-EIS and Stan-HMC samples of size $N = 1,000$ for the parameters of the Gamma volatility model in (27) and (28) applied to the American Express realized volatility data. The columns 'Min' and 'Mean' correspond to the minimum and mean across 8 independent replica of the experiment. Burn-in iterations are not included in the reported CPU times.

HMC tuning parameters we use $\varepsilon = 0.64$ and $L = 3$. In Figure 3 we provide the trace plots of the posterior MCMC samples for the parameters obtained from the resulting PM-HMC-EIS and the Stan-HMC together with the corresponding histograms and ACFs. The ACFs show that the autocorrelations for PM-HMC-EIS are very low and considerably smaller than those for Stan-HMC, revealing substantial gains in the mixing of the PM-HMC-EIS chains for the parameters. This is confirmed by the ESS values for the two procedures, which are reported in Table 2 together with the posterior means and standard deviations for the parameters. In fact, we find that the mean ESS for PM-HMC-EIS is between 1.9 (for β) and 5.8 (for ν) times larger than for Stan-HMC. This improvement in simulation efficiency gained by the PM-HMC-EIS appears to outweigh its higher computational costs relative to Stan-HMC, as it is indicated by the ESS/s values which are roughly of the same size for the two procedures.

Those results for the Gamma model together with the ones obtained for the SV model show that the simulation efficiency of PM-HMC-EIS for dynamic SSMs is fairly robust with respect to the signal-to-noise ratio and can have a competitive edge relative to standard HMC for joint sampling of the parameters and latent variables in applications where this ratio is large and data densities have as a function in the latent variables a shape depending on the parameters. This will be further illustrated in the next example where we consider an application with an extremely large signal-to-noise ratio.
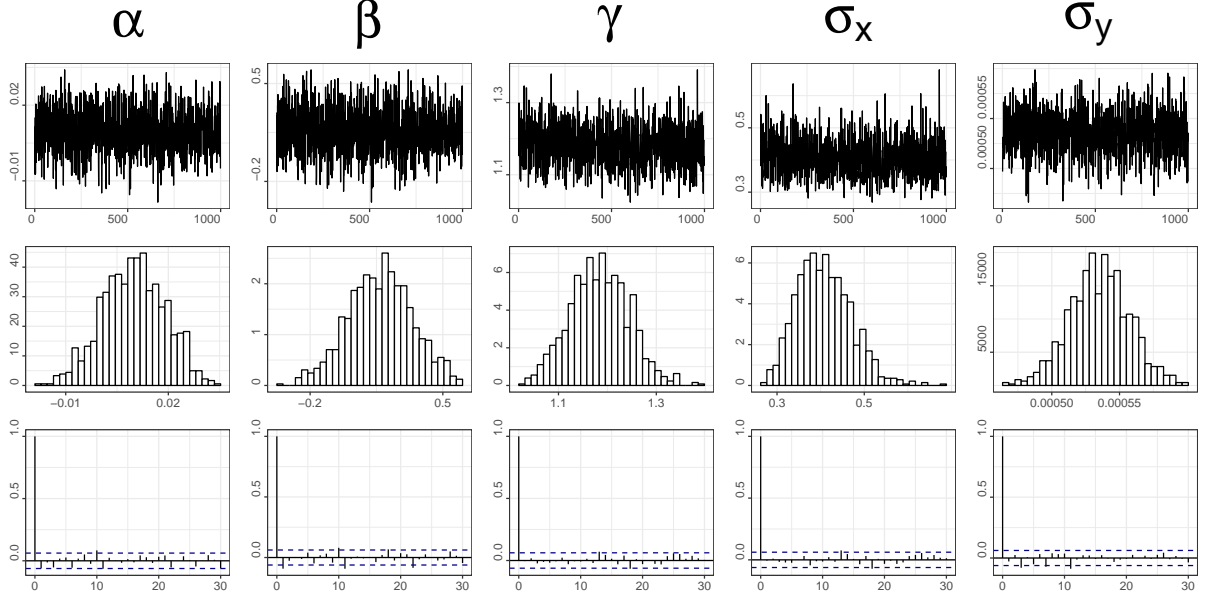
Figure 4: Trace plots (top), histograms (middle) and empirical autocorrelation functions (bottom) for a representative replica of PM-HMC-EIS applied to the CEV model in (29) and (30) for the Eurodollar interest rate data.

4.3 Constant Elasticity of Variance Diffusion Model

The last example model is a time-discretized version of the constant elasticity of variance (CEV) diffusion model for short-term interest rates (Chan et al., 1992), extended by a measurement error to account for microstructure noise (Aït-Sahalia, 1999; Kleppe and Skaug, 2016). The resulting model for the interest rate y_t observed at day t with a corresponding latent state x_t, is described as

$$y_t = x_t + \sigma_y e_t, \quad e_t \sim \mathrm{iid} N(0,1), \tag{29}$$

$$x_t = x_{t-1} + +\Delta(\alpha - \beta x_{t-1}) + \sigma_x x_{t-1}^\gamma \sqrt{\Delta} \eta_t, \quad \eta_t \sim \mathrm{iid} N(0,1), \tag{30}$$

where e_t and η_t are mutually independent and $\Delta = 1/252$. The parameters are $\boldsymbol{\theta} = (\alpha, \beta, \gamma, \sigma_x, \sigma_y)$ and the initial condition $x_1 \sim N(y_1, 0.01^2)$. The data we use consists of $T = 3,082$ daily 7-day Eurodollar deposit spot rates from January 2, 1983 to February 25, 1995 (see Ait-Sahalia, 1996 for a description of this data set). For α and β we assume Gaussian priors both with $N(0, 1000)$, for γ a uniform prior on the interval $[0, 4]$, and for σ_x^2 and σ_y^2 uninformative inverted-χ^2 priors with $p(\sigma_x^2) \propto 1/\sigma_x^2$ and $p(\sigma_y^2) \propto 1/\sigma_y^2$. The HMC computations are conducted on the following transformations of the parameters: $\boldsymbol{\theta}^* = (\alpha, \beta, \gamma, \log \sigma_x^2, \log \sigma_y^2)$.

In the interest rate data for this CEV model the estimated standard deviation of the noise component σ_y is very small with an estimate of 0.0005 (see Table 3) so that the data density $g_t(x_t, \boldsymbol{\delta})$ is strongly peaked at $x_t = y_t$ and by far more informative about x_t than in the SV and Gamma model with a Fisher information

		PM-HMC-EIS		MCRMHMC	
		Min	Mean	Min	Mean
	CPU time (s)	516.9	518.4		16200
	Acc. rate	0.92	0.93		
α	Post. mean		0.0099		0.0099
	Post. std.		0.009		0.0088
	ESS	872.7	979.2	1000	1000
	ESS/s	1.68	1.89	0.06	0.06
β	Post. mean		0.169		0.168
	Post. std.		0.172		0.172
	ESS	835.8	970.5	1000	1000
	ESS/s	1.61	1.87	0.06	0.06
γ	Post. mean		1.18		1.18
	Post. std.		0.06		0.06
	ESS	796.8	967.8	423	564
	ESS/s	1.54	1.87	0.03	0.04
σ_x	Post. mean		0.41		0.41
	Post. std.		0.06		0.06
	ESS	768.7	940.1	405	579
	ESS/s	1.49	1.81	0.03	0.04
σ_y	Post. mean		0.00054		0.00054
	Post. std.		0.00002		0.00002
	ESS	870.9	976.7	495	582
	ESS/s	1.67	1.88	0.03	0.04

Table 3: Posterior mean and standard deviation, ESS, ESS/s and acceptance probability of PM-HMC-EIS and Stan-HMC samples of size $N = 1,000$ for the parameters of the CEV model in (29) and (30) applied to the Euro-Dollar interest rate data. The columns 'Min' and 'Mean' correspond to the minimum and mean across the 8 independent replica of the experiment. Burn-in iterations are not included in the reported CPU times. The column MCRMHMC provides the results of a Riemann manifold Hamiltonian Monte Carlo algorithm for the same model and data set, reproduced from Table 4 of Kleppe (2018b). The MCRMHMC results were also implemented in C++ and were run on the same computer as used in this paper. The MCRMHMC results are based on 10 independent replica of $N = 1,000$ MCMC iterations.

given by $1/\sigma_y^2$. Also the volatility of the states is not constant and depends, unlike in the previous models, non-linearly on the level of the states. As a result the posterior of $\boldsymbol{\eta}$ and $\boldsymbol{\theta}$ strongly deviates from being Gaussian.

For the CEV model, only $J = 1$ EIS iteration based on a CRN sample size $r = 7$ is needed to obtain highly efficient EIS densities allowing us to set the simulation sample size for the likelihood approximations as in the previous applications to $n = 1$. The selection of the remaining tuning parameters are $\epsilon = 0.57$ and $L = 3$. Figure 4 shows the trace-plots, histograms and ACFs for the posterior samples of the parameters obtained using PM-HMC-EIS, and Table 3 reports the resulting posterior means and standard deviation as well as the ESS values. The results indicate that even in this challenging framework PM-HMC-EIS produces for all parameters close to perfect mixing MCMC chains. Owing to the extremely high signal-to-noise ratio of the model, Stan-HMC 'breaks down' and fails to produce meaningful results so that we refrain from reporting them. Instead, we report in Table 3 the results obtained from the modified Cholesky Riemann manifold Hamiltonian Monte Carlo (MCRMHMC) sampler (Kleppe, 2018b). Like the Stan-HMC, the MCRMHMC

procedure is an HMC for sampling on the joint space of parameters and latent states. However, while Stan-HMC uses only information in the first-order derivatives of the log target density in order to align the MCMC proposals with the local geometry of the target, MCRMHMC utilizes for this also the information provided via the Hessian. This makes the latter more robust with respect to strong nonlinear dependencies of the target variables under their joint posterior but also computationally substantially more expensive. Comparing the mean ESS values of PM-HMC-EIS with those of MCRMHMC, we find that for PM-HMC-EIS the lowest mean ESS value across the five parameters is 940 (for σ_x) while for MCRMHMC that lowest ESS value is 564 (for γ). Thus, PM-HMC-EIS is able to produce for a given number of MCMC draws a substantially larger amount of effective draws for the complete vector of parameters. Also when accounting for computing time and comparing the ESS/s values, we find that PM-HMC-EIS is roughly two orders of magnitudes faster in producing effective parameter draws.

5 Discussion of the $n = 1$ case

For the applications in the previous section we have found that the EIS density $m(\mathbf{x}|\mathbf{a}(\boldsymbol{\theta}))$ provides accurate likelihood estimates so that PM-HMC-EIS works very well with a simulation sample size as low as $n = 1$.

For this $n = 1$ case the PM-HMC target is according to (4) given by

$$\tilde{\pi}(\boldsymbol{\theta}, \mathbf{u}) \propto \mathcal{N}(\mathbf{u}|\mathbf{0}_D, \mathbf{I}_D) p(\boldsymbol{\theta}) \left[\frac{p(\mathbf{y}|\mathbf{x}, \boldsymbol{\theta}) p(\mathbf{x}|\boldsymbol{\theta})}{m(\mathbf{x}|\mathbf{a}(\boldsymbol{\theta}))} \right]_{\mathbf{x} = \gamma(\mathbf{a}(\boldsymbol{\theta}), \mathbf{u})}. \tag{31}$$

Assuming that the function γ defining the EIS sampling mechanism is bijective in $\mathbf{u}$ for each admissible $\boldsymbol{\theta}$, the change of variables implies that $\mathcal{N}(\mathbf{u}|\mathbf{0}_D, \mathbf{I}_D) = |\nabla_{\mathbf{u}} \gamma(\mathbf{a}(\boldsymbol{\theta}), \mathbf{u})| \left[m(\mathbf{x}|\mathbf{a}(\boldsymbol{\theta})) \right]_{\mathbf{x} = \gamma(\mathbf{a}(\boldsymbol{\theta}), \mathbf{u})}$, so that the target (31) can be rewritten as

$$\tilde{\pi}(\boldsymbol{\theta}, \mathbf{u}) \propto |\nabla_{\mathbf{u}} \gamma(\mathbf{a}(\boldsymbol{\theta}), \mathbf{u})| p(\boldsymbol{\theta}) \left[p(\mathbf{y}|\mathbf{x}, \boldsymbol{\theta}) p(\mathbf{x}|\boldsymbol{\theta}) \right]_{\mathbf{x} = \gamma(\mathbf{a}(\boldsymbol{\theta}), \mathbf{u})}. \tag{32}$$

For EIS samplers the bijectivity assumption is fulfilled under very mild conditions. It follows that the joint density for $(\boldsymbol{\theta}, \mathbf{x})$ which obtains from the PM-HMC target density for $(\boldsymbol{\theta}, \mathbf{u})$ by applying change of variables for $\mathbf{x} = \gamma(\mathbf{a}(\boldsymbol{\theta}), \mathbf{u})$ to (32) is the original joint posterior $p(\boldsymbol{\theta}, \mathbf{x}|\mathbf{y})$. This shows that PM-HMC sampling with $n = 1$ targeting (31) corresponds to standard HMC sampling targeting the joint posterior $p(\boldsymbol{\theta}, \mathbf{x}|\mathbf{y})$ reparameterized from $(\boldsymbol{\theta}, \mathbf{x})$- to $(\boldsymbol{\theta}, \mathbf{u})$-coordinates (Lindsten and Doucet, 2016). This relationship between the original joint posterior and the PM-HMC target together with its equivalent representations in (31) and (32) reveal a number of specific conceptual advantages of PM-HMC-EIS when the accuracy of EIS allows us

to reduce the simulation sample size to $n = 1$.

First, we notice that under the optimal IS density $m^*(\mathbf{x}|\boldsymbol{\theta}) = p(\mathbf{y}|\mathbf{x}, \boldsymbol{\theta})p(\mathbf{x}|\boldsymbol{\theta})/p(\mathbf{y}|\boldsymbol{\theta})$, which is approximated as close as possible by the EIS density $m(\mathbf{x}|\mathbf{a}(\boldsymbol{\theta}))$, the reparameterized joint posterior for $(\boldsymbol{\theta}, \mathbf{x})$ in (31) becomes

$$\tilde{\pi}^*(\boldsymbol{\theta}, \mathbf{u}) \propto \mathcal{N}(\mathbf{u}|\mathbf{0}_D, \mathbf{I}_D)p(\boldsymbol{\theta}|\mathbf{y}). \tag{33}$$

This implies that EIS implicitly aims at reparameterizing the joint posterior $p(\boldsymbol{\theta}, \mathbf{x}|\mathbf{y})$ to obtain a standard HMC target density in $(\boldsymbol{\theta}, \mathbf{u})$, where $\mathbf{u}$ is close to be standard normally distributed independent of $\boldsymbol{\theta}$ so that the Hamiltonian transition dynamics for $(\boldsymbol{\theta}, \mathbf{p}_{\boldsymbol{\theta}})$ is almost decoupled from that of $(\mathbf{u}, \mathbf{p}_{\mathbf{u}})$. Hence, for a given likelihood $p(\mathbf{y}|\boldsymbol{\theta})$ and prior $p(\boldsymbol{\theta})$, EIS is designed so as to make the PM-HMC target for $n = 1$ as well behaved as possible for an efficient HMC exploration of the joint space of $(\boldsymbol{\theta}, \mathbf{x})$ under their posterior. This explains why we have found in our applications close to perfect mixing MCMC chains for PM-HMC-EIS with $n = 1$. Reparameterizations aiming at producing more tractable target distributions for MCMC methods have a long tradition, and prominent examples are the affine reparameterizations common for Gibbs sampling applied to regression models (see, e.g., Gelman et al., 2014, Chapter 12). More recent examples include the optimal transport maps built from previous MCMC iterations as considered by Parno and Marzouk (2018) and, most closely related to the present work, the dynamically rescaled HMC approach of Kleppe (2018a), for which the PM-HMC-EIS reparameterization can be seen as a non-linear generalization.

Second, the correspondence between the PM-HMC target for $n = 1$ and the joint posterior $p(\boldsymbol{\theta}, \mathbf{x}|\mathbf{y})$ implies that whenever we have a sample $\{\theta^{(k)}, \mathbf{u}^{(k)}\}$ targeting (31), then $\{\theta^{(k)}, \gamma(\mathbf{a}(\theta^{(k)}), \mathbf{u}^{(k)})\}$ is targeting $p(\boldsymbol{\theta}, \mathbf{x}|\mathbf{y})$. Thus, draws from the smoothing distribution of the latent variables $p(\mathbf{x}|\mathbf{y})$ are available without additional computational costs.

Last but not least, the PM-HMC target for $n = 1$ tend to be fairly immune to the infinite-variance problem of IS procedures. As discussed, e.g., in Koopman et al. (2009), IS likelihood estimates such as that in (22) may have infinite variance and thus become unreliable, in particular in high-dimensional applications. This occurs when the tails of the IS density are thinner than those of the IS target distribution $p(\mathbf{x}|\boldsymbol{\theta}, \mathbf{y}) \propto p(\mathbf{y}|\mathbf{x}, \boldsymbol{\theta})p(\mathbf{x}|\boldsymbol{\theta})$, making the IS weight $\omega(\mathbf{x})$ unbounded as a function of $\mathbf{x}$. However, under the PM-HMC target (31) the EIS likelihood estimate is combined with the thin-tailed standard normal distribution of the variables $\mathbf{u}$ used to generate the IS estimate, which counteracts the potential unboundedness of the IS weight in the $\mathbf{u}$-direction.

This robustness of PM-HMC with respect to the infinite-variance problem is also evident in the representation of the PM-HMC target in (32), which does not involve the IS weight. For thin-tailed Gaussian EIS densities $m(\mathbf{x}|\mathbf{a}(\boldsymbol{\theta}))$ (as used for the applications in Sections 4.1 and 4.2) the function γ is affine so that the Jacobian determinant $|\nabla_{\mathbf{u}}\gamma(\mathbf{a}(\boldsymbol{\theta}), \mathbf{u})|$ is constant with respect to $\mathbf{u}$. Thus, for Gaussian EIS densities the

PM-HMC target obtains from an affine reparameterization of the latent variable $\mathbf{x}$, so that the tail behavior of (32) with respect to $\mathbf{u}$ will be the same as the tail behavior of $p(\boldsymbol{\theta}, \mathbf{x}|\mathbf{y})$ in $\mathbf{x}$. More general, for EIS densities including non-Gaussian ones (such as that used for the application in Section 4.3) it is the case that when they provide a good approximation to the optimal IS density $m^*(\mathbf{x}|\boldsymbol{\theta})$ then the PM-HMC target in (32) is close to the optimal one in (33) with a Gaussian tail behavior in $\mathbf{u}$.

6   Conclusions

The pseudo-marginal HMC (PM-HMC) is an MCMC procedure for approximating the posterior distribution of the parameters in non-Gaussian and/or non-linear latent variable models. It approximates the ideal HMC targeting the marginal posterior of the parameters by replacing the intractable likelihood of the data with an unbiased importance sampling (IS) estimate. As such PM-HMC is designed to improve the simulation efficiency of pseudo-marginal methods based on standard MH updating schemes for the parameters and standard HMC methods sampling on the joint space of the parameters and the latent variables. However, the efficiency of PM-HMC critically hinges on the accuracy of the likelihood estimates and sufficiently accurate estimates are often not attainable by standard IS procedures, especially in models with high-dimensional latent dependence structures such as in dynamic state-space models (SSM) for time series.

Here we have proposed to combine the PM-HMC approach with efficient importance sampling (EIS), which is designed to minimize the MC variance of IS likelihood estimates for a broad class of latent variable models. Applications to dynamic SSMs illustrate the potential of the combined PM-HMC-EIS algorithm, showing that it achieves a very high simulation efficiency by producing close to perfectly mixing MCMC chains from the posterior of the parameters, even in challenging scenarios with high and/or parameter dependent signal-to-noise ratios. Moreover, the high precision of EIS in estimating the likelihood ensures that PM-HMC-EIS works very well even with an IS-simulation sample size as low as $n = 1$. In the $n = 1$ case, PM-HMC reduces to standard HMC targeting a reparameterized version of the joint posterior for the parameters and the latent variables. The particular advantage of EIS in this case is that it makes the resulting reparameterization of the joint posterior as well behaved as possible for an efficient exploration by standard HMC sampling.

While we have focussed in this paper on univariate dynamic latent variable models for time series, the generic structure of the proposed PM-HMC-EIS indicates that it can easily be applied to dynamic latent variable models for multivariate time series as well as models with latent correlation structures for cross-sectional data including but not limited to discrete-choice probit models with correlated errors and non-Gaussian models with latent spatial correlation.

References

Ait-Sahalia, Y. (1996). Testing continuous-time models of the spot interest rate. *The review of financial studies 9*(2), 385–426.

Aït-Sahalia, Y. (1999). Transition densities for interest rate and other nonlinear diffusions. *The Journal of Finance 54*(4), 1361–1395.

Andrieu, C., A. Doucet, and R. Holenstein (2010). Particle Markov chain Monte Carlo methods. *Journal of the Royal Statistical Society: Series B (Statistical Methodology) 72*(3), 269–342.

Bauwens, L. and F. Galli (2009). Efficient importance sampling for ML estimation of SCD models. *Computational Statistics and Data Analysis 53*, 1974–1992.

Beskos, A., N. Pillai, G. Roberts, J.-M. Sanz-Serna, and A. Stuart (2013). Optimal tuning of the hybrid Monte Carlo algorithm. *Bernoulli 19*(5A), 1501–1534.

Betancourt, M. and M. Girolami (2015). Hamiltonian Monte Carlo for hierarchical models. *Current trends in Bayesian methodology with applications 79*, 30.

Blanes, S., F. Casas, and J. Sanz-Serna (2014). Numerical integrators for the hybrid Monte Carlo method. *SIAM Journal on Scientific Computing 36*(4), A1556–A1580.

Bos, C. S. and N. Shephard (2006). Inference for adaptive time series models: stochastic volatility and conditionally Gaussian state space from. *Econometric Reviews 25*(2-3), 219–244.

Chan, K. C., G. A. Karolyi, F. A. Longstaff, and A. B. Sanders (1992). An empirical comparison of alternative models of the short-term interest rate. *The Journal of Finance 47*(3), 1209–1227.

Danielsson, J. (1994). Stochastic volatility in asset prices: Estimation with simulated maximum likelihood. *Journal of Econometrics 64*, 375–400.

DeJong, D. N., R. Liesenfeld, G. V. Moura, J.-F. Richard, and H. Dharmarajan (2012). Efficient likelihood evaluation of state-space representations. *Review of Economic Studies 80*(2), 538–567.

Doucet, A., N. de Freitas, and N. Gordon (2001). *Sequential Monte Carlo Methods in Practice*. Springer.

Duane, S., A. D. Kennedy, B. J. Pendleton, and D. Roweth (1987). Hybrid Monte Carlo. *Physics letters B 195*(2), 216–222.

Durbin, J. and S. J. Koopman (2012). *Time Series Analysis by State Space Methods* (2 ed.). Number 38 in Oxford Statistical Science. Oxford University Press.

Eddelbuettel, D. and R. François (2011). Rcpp: Seamless R and C++ Integration. *Journal of Statistical Software 40*(8), 1–18.

Fernandez-Villaverde, J. and J. F. Rubio-Ramirez (2007). Estimating macroeconomic models: A likelihood approach. *Review of Economic Studies 74*(4), 1059–1087.

Flury, T. and N. Shephard (2011). Bayesian inference based only on simulated likelihood: particle filter analysis of dynamic economic models. *Econometric Theory 27*(Special Issue 05), 933–956.

Gelman, A., J. B. Carlin, H. S. Stern, D. B. Dunson, A. Vehtari, and D. Rubin (2014). *Bayesian Data Analysis* (3 ed.). CRC Press.

Geyer, C. (1992). Practical Markov chain Monte Carlo. *Statistical Science 7*(4), 473–483.

Golosnoy, V., B. Gribisch, and R. Liesenfeld (2012). The conditional autoregressive wishart model for multivariate stock market volatility. *Journal of Econometrics 167*(1), 211–223.

Griewank, A. (2000). *Evaluating Derivatives: Principles and Techniques of Algorithmic Differentiation.* SIAM, Philadelphia.

Grothe, O., T. S. Kleppe, and R. Liesenfeld (2018). The Gibbs sampler with particle efficient importance sampling for state-space models. *Econometric Reviews*. Forthcoming.

Harvey, A., E. Ruiz, and N. Shephard (1994). Multivariate stochastic variance models. *The Review of Economic Studies 61*(2), 247–264.

Hoffman, M. D. and A. Gelman (2014). The No-U-turn sampler: adaptively setting path lengths in Hamiltonian Monte Carlo. *Journal of Machine Learning Research 15*(1), 1593–1623.

Hogan, R. J. (2014). Fast reverse-mode automatic differentiation using expression templates in c++. *ACM Transactions on Mathematical Software (TOMS) 40*(4), 26.

Kleppe, T. S. (2017). Adaptive step size selection for hessian-based manifold Langevin samplers. *Scandinavian Journal of Statistics 43*(3), 788–805.

Kleppe, T. S. (2018a). Dynamically rescaled Hamiltonian Monte Carlo for Bayesian hierarchical models. arXiv:1806.02068.

Kleppe, T. S. (2018b). Modified Cholesky Riemann manifold Hamiltonian Monte Carlo: exploiting sparsity for fast sampling of high-dimensional targets. *Statistics and Computing 28*(4), 795–817.

Kleppe, T. S. and R. Liesenfeld (2014). Efficient importance sampling in mixture frameworks. *Computational Statistics & Data Analysis 76*, 449 – 463.

Kleppe, T. S. and H. J. Skaug (2016). Bandwidth selection in pre-smoothed particle filters. *Statistics and Computing 26*(5), 1009–1024.

Kleppe, T. S., J. Yu, and H. J. Skaug (2014). Maximum likelihood estimation of partially observed diffusion models. *Journal of Econometrics 180*(1), 73 – 80.

Koopman, S. J., N. Shephard, and D. Creal (2009). Testing the assumptions behind importance sampling. *Journal of Econometrics 149*(1), 2 – 11.

Leimkuhler, B. and S. Reich (2004). *Simulating Hamiltonian dynamics.* Cambridge University Press.

Liesenfeld, R. and J.-F. Richard (2003). Univariate and multivariate stochastic volatility models: estimation and diagnostics. *Journal of Empirical Finance 10*(4), 505–531.

Liesenfeld, R. and J.-F. Richard (2006). Classical and Bayesian analysis of univariate and multivariate stochastic volatility models. *Econometric Reviews 25*(2-3), 335–360.

Liesenfeld, R. and J.-F. Richard (2008). Improving MCMC, using efficient importance sampling. *Computational Statistics & Data Analysis 53*(2), 272–288.

Liesenfeld, R. and J.-F. Richard (2010). Efficient estimation of probit models with correlated errors. *Journal of econometrics 156*(2), 367–376.

Liesenfeld, R., J.-F. Richard, and J. Vogler (2016). Likelihood evaluation of high-dimensional spatial latent Gaussian models with non-Gaussian response variables. In R. K. P. Badi H. Baltagi, James P. Lesage (Ed.), *Spatial Econometrics: Qualitative and Limited Dependent Variables (Advances in Econometrics, Volume 37)*, Chapter 2, pp. 35–77. Emerald Insight.

Liesenfeld, R., J.-F. Richard, and J. Vogler (2017). Likelihood-based inference and prediction in spatio-temporal panel count models for urban crimes. *Journal of Applied Econometrics 32*(3), 600–620.

Lindsten, F. and A. Doucet (2016). Pseudo-marginal Hamiltonian monte carlo. *arXiv preprint arXiv:1607.02516*.

Liu, J. S. (2001). *Monte Carlo strategies in scientific computing.* Springer, Berlin.

Malik, S. and M. K. Pitt (2011). Particle filters for continuous likelihood evaluation and maximisation. *Journal of Econometrics 165*(2), 190 – 209.

Mannseth, J., T. S. Kleppe, and H. J. Skaug (2018). On the application of improved symplectic integrators in Hamiltonian Monte Carlo. *Communications in Statistics-Simulation and Computation 47*(2), 500–509.

Moura, G. V. and D. E. Turatti (2014). Efficient estimation of conditionally linear and Gaussian state space models. *Economics Letters 124*(3), 494 – 499.

Neal, R. M. (2011). MCMC using Hamiltonian dynamics. *Handbook of Markov Chain Monte Carlo 2*, 113–162.

Parno, M. and Y. Marzouk (2018). Transport map accelerated Markov chain Monte Carlo. *SIAM/ASA Journal on Uncertainty Quantification 6*(2), 645–682.

Pitt, M. K., R. dos Santos Silva, P. Giordani, and R. Kohn (2012). On some properties of Markov chain Monte Carlo simulation methods based on the particle filter. *Journal of Econometrics 171*(2), 134 – 151.

R Core Team (2018). *R: A Language and Environment for Statistical Computing*. Vienna, Austria: R Foundation for Statistical Computing.

Richard, J.-F. and W. Zhang (2007). Efficient high-dimensional importance sampling. *Journal of Econometrics 141*(2), 1385–1411.

Robert, C. and G. Casella (2004). *Monte Carlo methods* (2 ed.). Springer, Berlin.

Scharth, M. and R. Kohn (2016). Particle efficient importance sampling. *Journal of Econometrics 190*(1), 133 – 147.

Stan Development Team (2017). *Stan Modeling Language Users Guide and Reference Manual* (2.17.0 ed.).

Stan Development Team (2018). RStan: the R interface to Stan, Version 2.17.3. http://mc-stan.org.

Taylor, S. J. (1986). *Modelling Financial Time Series*. Wiley, Chichester.